https://doi.org/10.46813/2024-150-076

UDC 538.9:620.3:621.7

SYNTHESIS, STRUCTURE, AND PROTECTIVE PROPERTIES OF PVD MAX PHASE COATINGS. A REVIEW.
PART II. STRUCTURE, PROPERTIES, APPLICATION PROSPECTS

E.N. Reshetnyak[1], A.S. Kuprin[1], T.A. Prikhna[2], M.A. Bortnitskaya[1], V.A. Belous[1]
[1]National Science Center "Kharkov Institute of Physics and Technology", Kharkiv, Ukraine;
[2]V. Bakul Institute for Superhard Materials of the National Academy of Sciences of Ukraine, Kyiv, Ukraine
E-mail: reshetnyak@kipt.kharkov.ua

The unique hybrid properties of ceramics and metals due to their special nanolayer structure make MAX phases an attractive material for working in harsh environments. Successes in the development of PVD processes for the synthesis of nanocrystalline coatings of MAX phases at low temperatures on technologically important substrates open up significant prospects for their application. This part of the review is devoted to the properties of MAX phases that make them useful for creating multifunctional coatings to protect the surface of materials operating under difficult conditions of high temperature, corrosion, and radiation. The influence of PVD deposition parameters on the structure of MAX phase coatings is analyzed. The peculiarities of the mechanical and tribological properties of the coatings, their resistance to erosion, corrosion, and radiation, and their ability to self-repair damage at high temperatures are discussed. Prospects for the use of MAX phase PVD coatings in various industries and ways to improve their protective properties are considered.

INTRODUCTION

Surface modification technologies have attracted the attention of many researchers as an effective way to improve the complex properties of materials. In recent years, protective ceramic coatings made of MAX phases have gained popularity among many other composite coatings. MAX phases are nanolaminated hexagonal carbides and nitrides with the general formula $M_{(n+1)}AX_n$ (M: early transition metal; A: Group IIIA or IVA element; X: carbon or nitrogen; n = 1–3 or higher). They contain successive layers of octahedral $M_{n+1}X_n$ and pure A elements with covalent ionic bonds MX and metallic MA. The special nanometer layer structure and combined bonding type give MAX ceramic phases the advantages of both metallic and ceramic materials. As a result, they have a high Young's modulus, damage resistance and self-healing ability, resistance to high-temperature oxidation and radiation, corrosion resistance and wear resistance, combined with electrical conductivity and good thermal properties [1–4]. Therefore, the synthesis of MAX phases in the form of coatings is of increasing interest for many applications [5–9].

Successful development of MAX phase coatings requires an understanding of how the production method and deposition parameters affect the composition, crystallographic structure and morphology. In turn, it is important to know how they determine the physical, mechanical and technological properties of the resulting material. The purpose of this review is to summarize the progress made in the field of protective coatings based on MAX phases. The first part of this review [10] discusses the advantages and characteristics of the synthesis of such coatings using ion-plasma physical vapor deposition (PVD) methods. The purpose of this part is to consider the properties of MAX phases that make them useful for creating multifunctional coatings to protect the surface of materials operating under difficult conditions of high temperature, corrosion, and radiation. Special attention is paid to the influence of PVD deposition parameters on the structure and properties of coatings. The possibilities of obtaining coatings with high protective properties and prospects of their application in various industries are considered.

1. POTENTIAL AREAS OF APPLICATION FOR MAX PHASE COATINGS

The main characteristic of MAX phases is a unique combination of metallic and ceramic properties. Similar to metals, MAX phases are good conductors, with a resistivity of 0.02 to 2 μΩ·m at room temperature, which increases linearly with increasing temperature [2]. In some cases (Ti_3SiC_2 or Ti_3AlC_2), their conductivity is higher than that of pure metallic Ti. From a thermal point of view, MAX phases, like other conductors, have good thermal properties, with thermal conductivity from 26 to $60\ W\cdot m^{-1}\cdot K^{-1}$ at ambient temperature and more than $20\ W\cdot m^{-1}\cdot K^{-1}$ at high temperatures (~ 800 K). This value is sometimes higher than that of metals or alloys such as pure Ti and Zircaloy [11]. In addition, MAX phases are heat resistant and quite refractory, making them a promising material for various high temperature applications. At temperatures below 1000 °C, most MAX phases are structurally stable. In vacuum, the phase decomposition temperatures for bulk samples of Ti_2AlC, Ti_3AlC_2, and Ti_3SiC_2 range from 1500 to 2200 °C. In practice, the exact decomposition temperature depends on the presence of impurities and the chemical environment [12]. The coefficient of thermal expansion (CTE) of MAX phases is between that of oxygen-free ceramics and that of metals. Typically, the average CTE varies between $8 \cdot 10^{-6}$ and $10 \cdot 10^{-6}\,K^{-1}$, although some compositions have lower or higher values (Fig. 1,a) [2].

Similar to ceramic double carbides and MX nitrides, the MAX family of phases exhibits elastic stiffness with Young's and shear moduli in the range of 200…350 and 120…140 GPa, respectively. Combined with the fact that the density of most MAX phases is relatively low (4…5 $g \cdot cm^{-3}$), their specific stiffness can be quite high. For example, the specific stiffness of Ti_3SiC_2 is comparable to that of Si_3N_4 and about three times higher than that of Ti. The Poisson's ratios for all MAX phases fluctuate around 0.2, which is lower than the value of 0.3 for Ti and closer to 0.19 for nearly stoichiometric TiC. In general, the MAX phases containing In, Pb, and Sn are less stiff than those consisting of lighter A elements, especially Al. The effect of X variation on the elastic properties is less significant. A comparison of the experimental and theoretical values of Young's modulus (E) and bulk modulus (B) of the selected MAX phases is shown in Fig. 1,a. Several theoretical works have shown a correspondence between the modulus B of binary MX compounds and ternary MAX compounds, which is quite expected, since the latter consist of blocks of the former. In most cases, the agreement between the measured and calculated values of E and B is acceptable. However, there are exceptions. Theoretical calculations overestimate the elastic properties of Cr_2AlC. This overestimation may be due to the presence of vacancies in the measured samples. Interestingly, MAX phases exhibit nonlinear, hysteresis elastic behavior, which is unusual for rigid compounds. For example, polycrystalline Ti_3SiC_2 cyclically loaded in compression up to 1 GPa at room temperature fully recovers after the load is removed [13].

MAX phases, unlike their MX counterparts, are relatively soft and extremely damage tolerant. Vickers hardness values of MAX polycrystalline phases are in the range of 2…8 GPa. This can be explained by the easy sliding of the base plane due to the layered structure and the relatively weak bond between the MX and A layers. Thus, MAX phases are softer than most structural ceramics, but harder than most metals. Single crystal studies have shown that the hardness of MAX phases is anisotropic and has a higher value when loaded along the *c* direction [11, 13].

The layered structure implies a good tribological response. An ultra-low coefficient of friction (μ) has been measured for the basal planes of Ti_3SiC_2 (0.002…0.005) using a scanning force microscope. However, the results published later for polycrystalline samples are not as impressive. In general, the initial μ value at room temperature was low (< 0.2) but quickly increased to higher values (> 0.4). The wear rate was relatively high and almost linearly dependent on the sliding distance. In addition, the tribological response of polycrystalline MAX phases is controlled by complex tribochemical reactions and depends on many factors: microstructure (grain size, purity, porosity), counterbody (metal, ceramic), and test conditions (temperature, atmosphere, speed, pressure, lubrication). It has been found that the tribological properties of MAX phase samples can be improved by the addition of a secondary phase such as Al_2O_3, BN, B_4C, SiC, Ti_5Si_3, and Ag [2].

MAX phases retain good mechanical properties even at elevated temperatures. The mechanical response at elevated temperatures is particularly interesting because of the brittle-to-plastic transition around 1000…1100 °C, depending on composition and microstructure. Below this transition temperature, some MAX phases are brittle like ceramics, but above it, they are ductile with strain at break up to 25%. Most ceramics are susceptible to thermal shock damage because of their brittleness. The response of MAX phases to thermal shock is different from other ceramics. As a result, Ti_3AlC_2 and Ti_3SiC_2 exhibit excellent resistance to thermal shock, which is associated with the formation of compressive stresses in the surface oxide layer, the presence of a metallic nature of the compound, and the formation of bands of kinks [2, 6, 12].

In addition to high temperature resistance, many MAX phases are highly resistant to radiation damage. The compounds Ti_3SiC_2, Ti_2AlC, Ti_3AlC_2, Cr_2AlC, V_2AlC, Zr_2AlC, Zr_3AlC_2, and Nb_4AlC_3 have been proposed as materials for nuclear power because of their good radiation tolerance at room and high temperatures [2, 12]. Upon irradiation with heavy ions, elastic collisions and electronic interactions were found to lead to unit cell expansion along the c-axis, grain boundary sputtering, and selective sputtering as a function of crystal orientation, crystal structure transformation, and amorphization of MAX phases [14]. When irradiated in the range up to 0.1 dpa, Ti_2AlC and Ti_3SiC_2 phases show good recovery dynamics, and elevated temperatures provide sufficient migration energy and recombination of point defects and damage annealing. The MAX phase of Ti_3AlC_2 shows excellent tolerance to irradiation. Amorphization does not occur up to 31 dpa, although the nanolamellar structure disappears due to defect formation and the phase transition from α to β Ti_3AlC_2 phase. Similar phase transitions from the HCP to the FCC structure have been found in Ti_2AlN, Ti_2AlC and Ti_4AlN_3 [2, 12]. In addition, MAX phases based on Zr and Nb have recently appeared, which are promising due to the small neutron cross section of Zr and the favorable properties of refractory Nb. After irradiation, Zr_3AlC_2 and $(Zr_{0.5,}Ti_{0.5})AlC_2$ were found to have excellent defect repair capability above 400 °C [15, 16].

In terms of oxidation resistance, not all MAX phases behave in the same way, since the oxidation process depends mainly on the elemental composition. The most promising MAX phases are those containing Al, which form a continuous, dense and thermodynamically stable protective layer of thermally grown oxide (TGO) containing aluminum oxide (α-Al_2O_3) on the surface. The highly adhesive TGO layer effectively protects against further diffusion of oxygen inside at temperatures up to 1400 °C [17]. Unfortunately, not all Al-based MAX phases form an outer protective layer of alumina, which is related to the competition between oxidation of "M" and "A" elements. The Ti_2AlC, Ti_3AlC_2, and Cr_2AlC phases form protective Al_2O_3 layers, but V_2AlC, Ta_2AlC, and Nb_2AlC [18, 19] preferentially form M-oxides such as V_2O_5, Ta_2O_5, and Nb_2O_5, respectively, on the surface. Thus, the MAX phases Ti_2AlC, Ti_3AlC_2, and Cr_2AlC are considered the most efficient for operation in aggressive environments at high temperatures (900…1400 °C) for long periods of time in both air and humid atmospheres. However, the oxidation reaction is strongly influenced by structural factors such as particle size, orientation, secondary phases (carbides and intermetallics), Al/M ratio and surface roughness [2]. Many MAX phases, such as Ti_3SiC_2, Ti_3AlC_2, Ti_2AlC, and Cr_2AlC, have shown excellent corrosion resistance to various environments, including molten Pb, Na, and Pb-Bi alloys, molten Na_2SO_4 and KNO_3-$NaNO_3$ salts, aqueous solutions of NaCl, H_2SO_4, and HCl [2, 11, 20–22].

In recent years, the Cr_2AlC system has attracted much attention mainly because of its excellent resistance to high-temperature oxidation and hot corrosion [23], as well as its low phase formation temperature. It has been found that Cr plays no less an important role than Al in the formation of a protective oxide layer. In addition, Cr_2O_3 formed as a result of Cr oxidation has a lubricating effect at high temperatures, making Cr_2AlC a potential material for applications requiring resistance to high-temperature wear. An additional advantage of Cr_2AlC over other MAX phases is that its thermal expansion is close to that of most process alloys and metal oxides, which not only ensures good adhesion of coatings at the coating/substrate and coating/protective oxide interfaces, but also prevents the possibility of coating cracking during operation [6–8, 24].

Achieving chemical diversity and controlling the performance of MAX phases largely depends on solid solution based approaches. It has been found that for some systems, the solid solution deviates from Wegard's law and the best performance can be achieved in the solid solution [25].

Due to the set of properties described above, coatings based on MAX phases are being actively considered for use as multifunctional coatings.

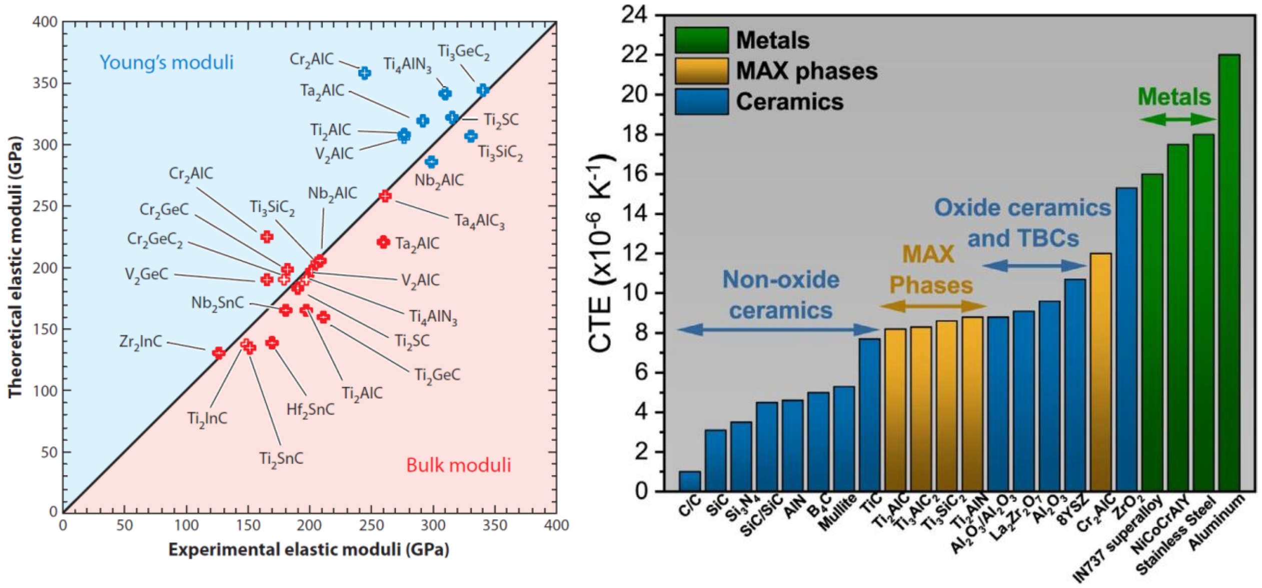

a *b*

Fig. 1. Comparison of experimental and theoretical elastic moduli of selected MAX phases (a) [13] and thermal expansion coefficients (TEC) of ceramics, MAX phases and metals (b) [2]

PVD deposition methods allow the synthesis of MAX phase coatings at temperatures hundreds of degrees below the synthesis temperature of the bulk material, which significantly expands the possible areas of application. Thin layers of MAX phases with a thickness of 500…800 nm are promising for use in small areas and moderate loads, such as sliding electrical contacts, sensors, anode materials, thin damping layers of microelectromechanical systems MEMS, ohmic contacts for high temperature power electronics [5, 9, 11, 26, 27]. Recently, due to the successes in the development of PVD processes for the synthesis of thicker coatings on various types of substrates, it has been shown that MAX phase coatings can be effectively used for the comprehensive protection of substrates under such harsh conditions as high temperature, corrosion, and radiation [2, 4, 5, 8, 9, 12, 24, 28–31]. Highly resistant protective coatings for titanium, aluminum, zirconium alloys, steels, and nickel-based superalloys are being actively developed and are important for the aerospace, automotive, marine, chemical, and nuclear industries.

The most promising areas of application for MAX phase protective coatings include:

– high-temperature coatings for the protection of gas turbine engine parts and components;

– bonding layers in thermal barrier coatings (TBC);

– joint coatings for solid oxide fuel cells;

– coatings for accident tolerant fuel (ATF) cladding of nuclear reactors;

– radiation-resistant coatings for nuclear power materials;

– oxidation/corrosion and erosion resistant coatings for titanium, aluminum and nickel alloys;

– coatings for protection against solar radiation;

– high-temperature tribological coatings.

Extreme operating conditions require careful selection of coating composition, process, and deposition parameters. It is well known that the properties of coatings can differ significantly from those of the same bulk material. The properties of PVD coatings are significantly influenced by structural characteristics such as impurities, phase purity, morphology, grain size, crystal defects, texture, stresses and substrate adhesion, which can vary significantly depending on the deposition parameters. In addition, the properties of coatings can vary with thickness [32]. Thus, identifying the relationships between PVD deposition parameters, structure, and properties of MAX phase coatings is an urgent need for the implementation of these materials in various fields.

2. INFLUENCE OF PVD DEPOSITION PARAMETERS ON THE STRUCTURE OF MAX PHASE COATINGS

The growth mechanisms, structure formation, morphology, texture and properties of ion plasma PVD coatings can vary significantly depending on many interrelated synthesis process parameters. Cathode composition, flux density, degree of ionization, gas composition and pressure, bias potential, and substrate temperature or distance to the substrate all affect the growth processes. Each of the process parameters has an ambiguous effect on the composition and structure of the coatings, and it is impossible to smoothly change the properties of the synthesized coatings by changing one of the process parameters, which makes it difficult to find new coating materials and deposition methods [32, 33]. MAX phase based coatings are no exception. The most studied parameter affecting the structure of MAX phases is the substrate temperature. The advantage of PVD coating deposition methods is that MAX phases can be synthesized at much lower temperatures than in bulk materials, but other coating deposition parameters are equally important [5, 6].

The effect of temperature on the synthesis of MAX phases in coatings was discussed in the previous part of this review [10]. It should be noted that a significant part of the work on the synthesis of MAX phase coatings has focused on the epitaxial growth of coatings on single crystal MgO or Al_2O_3 substrates [9]. Wilhelmsson et al. first reported the epitaxial growth of thin films of the MAX phases Ti_2AlC and Ti_3AlC_2 by magnetron sputtering [34]. They grew films of high crystalline quality at 900 °C on Al_2O_3 (0001) substrates with a TiC (111) etch buffer layer to enhance the epitaxy [35]. Subsequent studies have shown that MAX phase thin films can be nucleated directly on the substrate [5, 36]. Later, many epitaxial films of different systems have been synthesized: Ti_2AlC, Ti_2GeC, Ti_2AlN, Cr_2GeC, Cr_2AlC, $(Ti,Zr)_2AlC$, $(Cr,Mn)_2AlC$, $(Mo,Mn)_2GaC$, $(Cr,Mn)_2GaC$, Ti_3AlC_2, Ti_3SiC_2, Ti_3GeC_2. The temperature required for the formation of MAX phases was determined by epitaxial conditions [9].

The change in the structure of coatings from polycrystalline to monocrystalline as a function of substrate temperature can be clearly studied using the example of Ti-Al-N films deposited on MgO (111) substrates by reactive magnetron sputtering [37]. At a temperature of 500 °C a mixture of Ti, Al and a cubic solid solution of (Ti,Al)N is formed in the film. Increasing the substrate temperature to 600 °C leads to the formation of the seeds of the polycrystalline MAX phase of Ti_2AlN, whose crystallinity is further improved by increasing the temperature to 700 and 720 °C. Finally, at 750 °C, a thin single-crystal Ti_2AlN (0002) film is formed, which has a characteristic layered hexagonal surface morphology, high hardness, high Young's modulus, and low electrical resistance. The mechanism of microstructure evolution with increasing temperature is discussed by the authors in terms of surface energy, lattice mismatch, and enhanced diffusion of adatoms at high growth temperatures. To date, the structure and properties of polycrystalline films of sufficient thickness (at least a few micrometers) for surface protection have been studied much less than epitaxial films.

It is advisable to synthesize protective polycrystalline coatings of MAX phases at relatively low substrate temperatures that cannot adversely affect the substrate material. During PVD deposition of coatings, the synthesis temperature is lowered by an additional energy flux resulting from the bombardment of the growth surface with energy particles. The effect of the bias voltage on the substrate, which determines the energy of the particles during deposition, has been less thoroughly studied than temperature, but there is evidence that there is a certain range of voltages, depending on the characteristics of the ion-plasma flow deposited on the substrate, that is optimal for the synthesis of MAX phase coatings [5]. As mentioned in the first part of this review, the value of the voltage can affect the elemental composition of the coatings due to the selective sputtering of light elements [10]. However, even if the appropriate elemental composition of the coating is maintained on the substrate surface, a low or too high bias voltage can negatively affect the quality of the coating.

In [38], the effect of changing the negative bias voltage of the substrate from 60 to 120 V on the properties of Cr_2AlC-based coatings obtained by DC magnetron sputtering at a substrate temperature of 560 °C was studied. It was found that all the coatings exhibited a dense columnar structure with a corresponding surface morphology. The columnar nanosized grains grow at an angle of 60…70 degrees relative to the substrate surface. As the voltage increases due to increased ion bombardment, the thickness of the coatings decreases from 9 to 7 μm, the angle of the columnar grains changes, and undesired carbide and intermetallic phases appear. The surface roughness of the coating and the size of the MAX phase crystallites change non-monotonically. The coating deposited at 90 V has the lowest roughness and crystallite size of 33 and 76 nm, respectively.

Changing the power of the magnetron sputtering can also affect the substructural properties of the coatings. In [39], a comparative study of Cr_2AlC coatings deposited at different average HiPIMS powers was performed, where the effect of pulse duration (20…60 μs) was found to be more effective than frequency (1.2…1.6 kHz). The results of the study showed that increasing the power in the range of 110…440 W increased the deposition rate of amorphous layers by 3.5 times. Annealing transformed all amorphous Cr-Al-C coatings to the polycrystalline MAX phase Cr_2AlC. With increasing power, the Al content, the surface roughness of the coatings, and the size of the MAX phase nanocrystallites decreased, but these changes were not significant enough to change the mechanical properties of the coatings significantly.

The structure of Cr_2AlC coatings as a function of DCMS power at a substrate voltage of 60 V was studied in [40]. Fig. 2 shows electron microscopic images of the cross-section and surface of the coatings deposited on nickel-chromium alloy substrates and Si (100) wafers at different powers ranging from 1.5 to 4.5 kW. The coatings, which were 5…9 μm thick, had a columnar nanocrystalline substructure with a column width of 200…500 nm. The column diameter increased slightly from the substrate to the coating surface. With increasing power, the slope of the columns relative to the substrate surface disappeared and the re-nucleation of the columns was observed, the locations of which are indicated by arrows in the Fig. 2,e,g. The authors consider this re-nucleation as a density defect when the ion energy becomes sufficiently high. It should be noted that in the floating potential of the substrate, when the ion energy was too low, the columns were also perpendicular to the surface [29, 39] and intercolumn pores were present [29].

In general, MAX phase coatings synthesized in a single step directly during the deposition process are characterized by a dense columnar structure [29, 38–41], corresponding to Zone 2 on the Anders diagram [42]. This structure is formed by ion bombardment and elevated substrate temperature. Two-step MAX phase coatings exhibit both columnar and equilibrium morphologies. In a two-step deposition, metastable coatings of appropriate composition, often amorphous, are deposited in the first step at low substrate temperature, and the synthesis of MAX phases occurs in the second step – vacuum annealing of the samples. Typically, MAX phase coatings follow the morphology of the metastable layer. For example, for the Cr_2AlC MAX phase, DC magnetron deposited films follow the columnar structure [43–45], and films obtained by HiPIMS [44, 45] and the combined method [24, 46] follow the equilibrium structure.

In [24], Cr_2AlC and $(Cr,V)_2AlC$ coatings with a thickness of about 7.5 μm were obtained by a combined deposition method of magnetron and vacuum arc, followed by annealing of the samples at 700 °C. The substrates were a nickel-based superalloy and a WC-Co carbide. A Cr interlayer was used to increase adhesion and to avoid mutual diffusion of elements between the coating and the substrate. The amorphous layers synthesized in the first step did not show columnar structure. Fig. 3 shows the electron microscopic images of the surface and cross section of the samples after the formation of the MAX phase of Cr_2AlC and solid solutions of $(Cr,V)_2AlC$ with different compositions. It can be seen that the coatings have a dense microstructure with macroparticles of cathode material, which is emitted by the cathode in vacuum arc deposition. As the V content increases, the number of macroparticles on the surface of the coating increases, resulting in an increase in roughness from 22 to 187 nm. This can be explained by a significant decrease in the melting point of the Cr cathode with the addition of V. The cross-sectional images show that the macroparticles are found only on the surface and are not present in the core of the coating, as they tend to exfoliate due to ion bombardment of the growth surface. Despite the annealing and phase transformation, there are no visible voids throughout the depth of the coatings, and the coating adheres strongly to the substrate. The cross-sectional morphology of all samples shows a dense, homogeneous nanostructure with no evidence of columnar structure. It is clear that the properties of coatings with columnar and equilibrium structures can be very different.

Another factor that can significantly affect the properties of PVD coatings is texture, which is particularly important for MAX phases, which belong to the hexagonal crystal system with significant property anisotropy. Epitaxial films of MAX phases typically grow with the basal planes (0001) in the coating plane, i.e., the c-axis of the hexagonal lattice coincides with the growth direction [34, 35, 47–55]. MAX phases of Ti-Al-C, Cr-Al-C, V-Al-C, and Ti-Al-N systems with different crystal phase orientations: (110), (103) (100), (001) have been synthesized in polycrystalline layers by different PVD deposition methods [6, 30, 38, 40, 56–58]. It is well known that the formation of texture in coatings deposited by energy ion fluxes is considered in the context of stresses and is related to the attempt to minimize the free energy of the system, which consists of strain energy and surface energy [59, 60]. For MAX phases (space group $P6_3/mmc$), the (0001) basal plane is the most stable orientation due to the lowest surface energy [61]. Under non-equilibrium conditions of PVD film growth at low temperatures, when the role of film deformation increases due to inhibition of relaxation processes, other orientations may be more energetically favorable.

Process parameters such as pressure, temperature and substrate voltage influence the preferred orientation. In [6, 58], the effect of deposition parameters on the morphology and texture of HiPIMS Cr-Al-C coatings deposited on Al_2O_3 substrates was investigated. The coatings had a columnar structure of the polycrystalline MAX phase of Cr_2AlC with the addition of a solid solution of $(Cr,Al)_2C_x$. An unusual preferential orientation (110) of the MAX phase crystallites was found, i.e. the basal planes (0001) were perpendicular to the substrate surface and the c-axis of the hexagons was in the plane of the coating. A schematic representation of the crystal texture and an SEM cross-section of one of these coatings are shown in Fig. 4,a,b. At a substrate temperature of about 400 °C, regardless of the applied bias voltage (60 or 100 V) and process pressure (300…900 mPa), the coatings had a columnar morphology and texture (0001). At low pressure and high voltage, which provided high ion bombardment energy, it was a dense and fine-grained structure (see Fig. 4,f,h). At high pressure and low voltage, i.e. low ion energy, it was porous and coarse-grained (see Fig. 4,g,i). In addition, a decrease in substrate temperature during deposition, combined with an increase in voltage and a decrease in process pressure, resulted in high residual stresses in the coating, which significantly affected the mechanical and adhesion properties of the coatings.

Texture can also be present in MAX phase coatings obtained by a two-step annealing process [6, 39, 45, 62]. Interestingly, the authors in [62] attribute the formation of texture in Cr-Al-C coatings to the influence of a Cr-C transition sublayer deposited on the substrate prior to coating. As a result of annealing, a polycrystalline MAX phase of Cr_2AlC was formed in an amorphous coating with a thickness of ~ 4 µm, and the transition layer was identified as Cr_3C_2. It was found that increasing the thickness of the transition layer from 0.8 to 2.3 µm leads to a change in the predominant orientation in the coatings from (002) to (103). Although, in our opinion, the texture analysis in most works requires a more thorough analysis. The peaks (103) and (006) of the MAX phases of the Cr_2AlC type practically overlap, forming a common peak, and the redistribution of intensity between (002) and (006) may be related to the order of the layers. As for the stress level, the advantages of the two-step deposition method include the possibility of relieving excessively high compressive stresses that accompany the crystallization of the amorphous phase in the annealing stage [26].

The results obtained indicate the importance of optimizing PVD processes for the deposition of thick polycrystalline MAX phase coatings at low temperatures on technologically important substrates made of metals and alloys. By varying the deposition parameters, the nanostructure of the films can be controlled over a wide range. In contrast to phase-pure epitaxial films, such polycrystalline coatings often contain a small amount of intermetallic, carbide/nitride, or amorphous phases in addition to the main MAX phase, which can affect their properties.

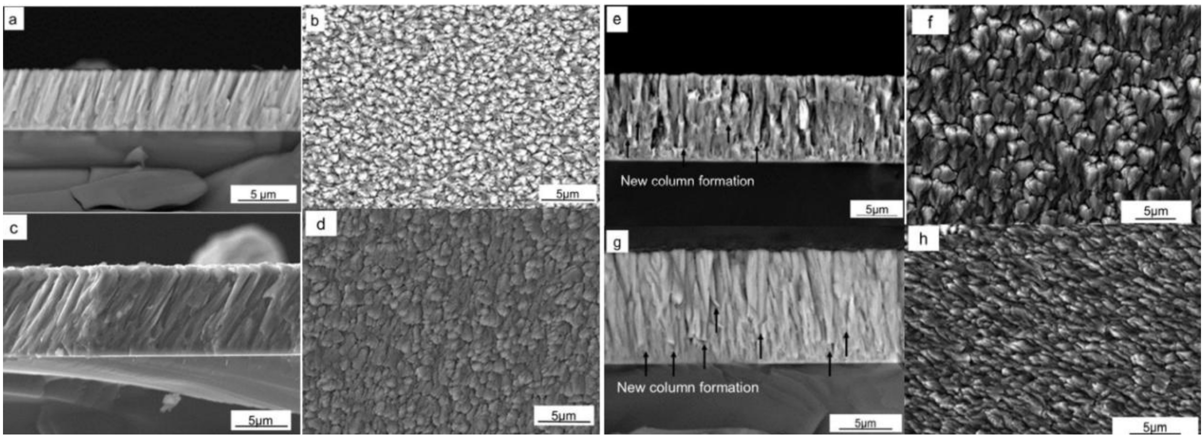

Fig. 2. Cross-sectional morphology (a, c, e, g) and surface morphology (b, d, f, h) of samples with MAX phase Cr_2AlC coatings applied at different magnetron sputtering power: 1.5 (a, b); 2.5 (c, d); 3.5 (e, f); 4.5 kW (g, h) [40]

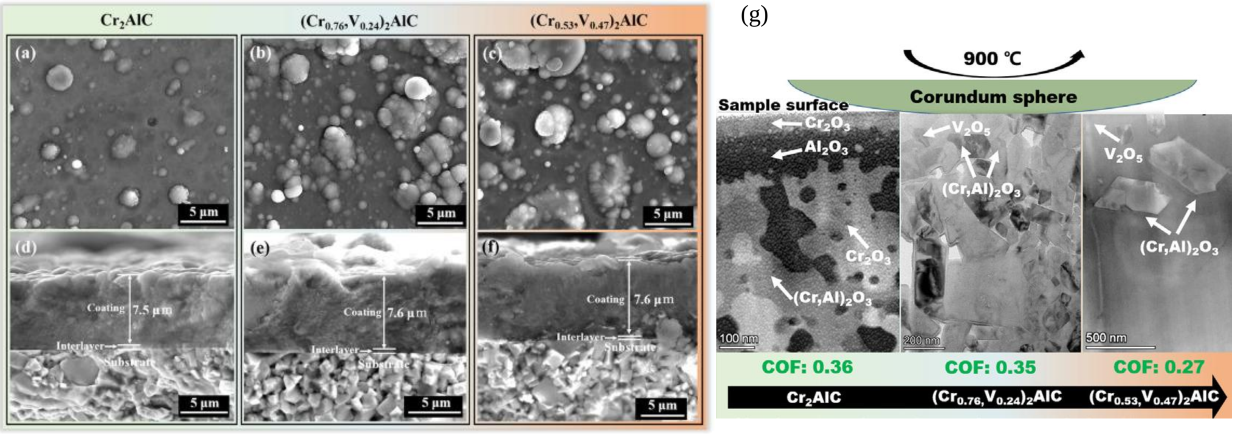

Fig. 3. Surface morphology (a, b, c) and cross-section (d, e, f) of samples coated with MAX phase Cr_2AlC and solid solutions of $(Cr,V)_2AlC$ of different composition obtained by the combined cathodic arc/magnetron deposition method followed by annealing. Cross-sectional images of the wear tracks of the coatings after tribological tests in the ball/disk scheme, carried out at 900 °C, with the coefficients of friction (g) indicated [24]

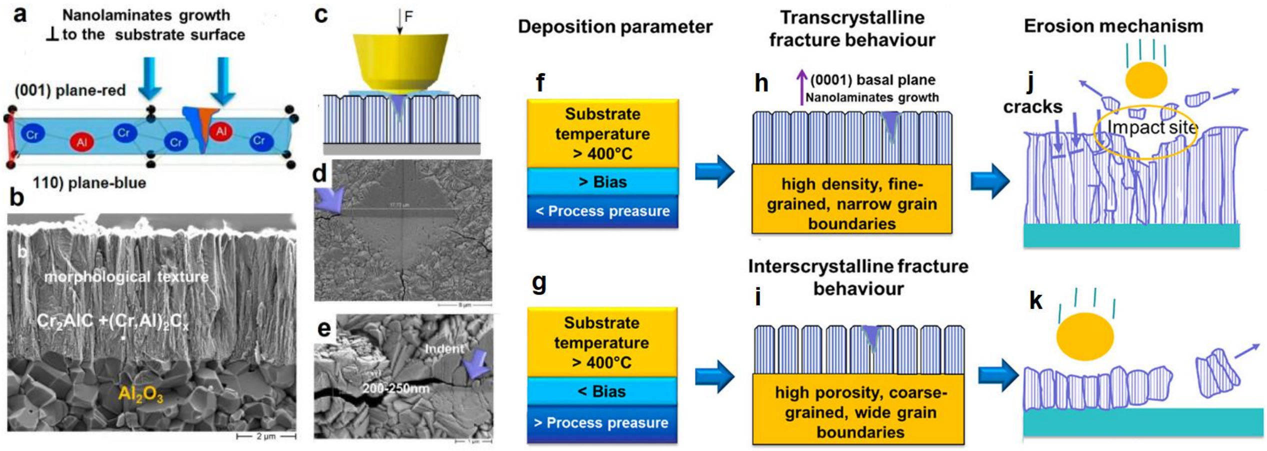

Fig. 4. Schematic representation of the crystal texture of the Cr$_2$AlC coating deposited by HPIMS (a). SEM image of the cross section of the coating (b). Schematic image of Vickers indentation (c). SEM image of Vickers indentation with a load of 200 g (d). Crack propagation on the surface of the coating after indentation (e). Schematic representation of the correlation between the deposition parameters of HiPIMS (f, g), the structure (h, i), and the mechanism of coating fracture during the wear resistance test (j, k) [6]

3. INFLUENCE OF PVD DEPOSITION PARAMETERS ON THE PROPERTIES OF MAX PHASE COATINGS

3.1. MECHANICAL PROPERTIES

The nanoindentation method is used to determine the hardness (H) and elastic modulus (E) of thin films and coatings. Calculations are performed on the basis of experimental load-unload curves in the coordinates load depth of indenter penetration. A peculiarity of load curves for epitaxial films of MAX phases is the presence of so-called “pop-in events” – horizontal sections on the curve corresponding to sudden penetration of the indenter under constant load, which is associated with the peculiarities of deformation of MAX phases due to shear and delamination with the formation of kinks bands [5, 63]. The curves reported in the literature for polycrystalline PVD coatings of the MAX phases do not contain such “pop-in” regions and show smooth behavior [24]. Hardness values for coatings of various systems are significantly higher than for the corresponding bulk MAX phases [5, 64]. This increase is typical of nanostructured ceramic coatings obtained under non-equilibrium PVD deposition conditions. The strengthening is associated with a combination of several factors, in particular nano-sized grains (Hall-Petch effect), crystal structure defects, compressive residual stresses, the presence of additional phases, etc. [65]. Table 1 shows the values of hardness and elastic modulus based on the results of nanoindentation of nanocrystalline coatings of some MAX phases. It can be seen that the discrepancy between the data is quite significant, which is due to both the composition of the coating (the strength of the chemical bonds of the phase) and the differences in structure. For example, the hardness and Young's modulus of Cr$_2$AlC coatings obtained by HiPIMS have higher values compared to those obtained by DCMS due to the denser morphology resulting from the enhanced ion bombardment [39]. Sometimes a correlation is noted between the smallest crystallite size and the highest hardness of coatings [38, 56]. On the example of Cr$_2$AlC coatings, it was found that the change in power during DCMS [40] or HiPIMS [39] deposition has little effect on the results of nanoindentation, and the change in voltage on the substrate, on the contrary [38].

Hardness and elasticity are equally important in improving wear resistance, especially in complex processes involving friction, impact and erosion. Since it is empirically known that the higher the hardness and Young's modulus, the lower the ability of coatings to deform and absorb energy before failure, it is desirable to increase both the hardness of the MAX phases and the toughness. The H/E ratio is often used to characterize the resistance of a material to elastic fracture deformation in an effort to increase this indicator [65]. For most of the coatings considered, the H/E parameter is in the range of 0.06…0.07, which is typical for wear-resistant ceramic coatings and indicates high mechanical properties (see Table 1).

The mechanical properties of the coatings can be further improved by solid solution hardening. By the combined deposition method, coatings of MAX phases of Cr$_2$AlC and solid solutions of (Cr,V)$_2$AlC with different V contents were obtained (see Fig. 3). The results showed that, compared with the Cr$_2$AlC coating, the hardness and Young's modulus of the (Cr$_{0.53}$,V$_{0.47}$)$_2$AlC coating increased by 34 and 24%, respectively, and the H/E parameter did not change significantly from 0.065 to 0.067. Nevertheless, the addition of V improved the behavior of the rather brittle Cr$_2$AlC coating on WC-Co carbide substrates in the scratch test. At a constant load of 19 N, the scratch morphology changed from extensive peeling to sporadic with a significantly smaller number and size of delaminated fragments, indicating an increase in fracture toughness and improved adhesion [24].

A scratch test of Ti$_3$AlC$_2$ coatings on SUS304 substrates showed that the coating with the highest MAX phase content had the highest H/E value and the lowest stress level, providing better adhesion with a critical load of 28 N [26]. It should be noted that the hardness of PVD coatings based on MAX phases is significantly affected by the presence and type of additional phases. In particular, if we consider a two-step synthesis method, during the annealing of amorphous layers, the hardness increases as the content of MAX phase increases. It is expected that the presence of hard cubic carbides will additionally increase the hardness and intermetallics will decrease it [26, 44, 56].

In addition to scratch testing, microscopic indent analysis after Vickers indentation (loading force ~ 2 N) is used to study the adhesion and fracture characteristics of coatings. Fig. 3,c,d show the indentation scheme and SEM images of the imprints after indentation of the Cr_2AlC coating with columnar morphology and strong texture (110). It can be seen that quite deep cracks of different widths and lengths appear near the corners of the indentation. These images are similar to those obtained for brittle fine-grained bulk Cr_2AlC ceramics [66]. The coatings exhibited transcrystalline fracture behavior, with cleavage of the layered Cr_2AlC grains occurring mainly parallel to the hexagonal reference plane (0001), as shown in Fig. 3,a. The crystallographic texture (110) is responsible for the formation of vertical cracks, which propagate mainly along the strong MX layers.

A completely different behavior during indentation is shown by non-textured Cr_2AlC, Ti_2AlC, V_2AlC coatings with equilibrium morphology [44, 56]. Dense coatings with a high content of the MAX phase (at least 90%) showed excellent toughness, in contrast to the brittle bulk analogues of the MAX phases. In general, MAX phases undergo a transition from a brittle to a plastic state at high temperatures, probably due to a decrease in grain size during deformation at high temperatures. The authors of [56] consider that coatings of MAX phases can exhibit excellent strength at lower temperatures precisely because of their fine grains. This is supported by the results of [64]. Among the coatings obtained by annealing amorphous magnetron layers, composites with nanosized (50…100 nm) MAX phase V_2AlC crystallites in an amorphous carbon matrix had the highest hardness, Young's modulus, H/E ratio, and the lowest fracture after Vickers indentation. Coatings composed mainly of the MAX phase had significantly poorer properties because they had a less compact structure and consisted of large lamellar grains with an average size of ~ 0.5 μm.

It should be noted that the mechanical properties of coatings may change slightly at high temperatures due to the gradual decomposition of the MAX phase. It has been observed that FCAD coatings of Ti_3AlC_2 begin to decompose at temperatures above 800 °C [26]. Increasing the amount of TiC carbide in the coating actually results in a slight strengthening of the coatings, but their brittleness and stress level increase. In Cr_2AlC magnetron coatings, similar decomposition can begin as early as 750 °C [6, 39].

Table 1

Results of nanoindentation of nanocrystalline coatings based on MAX phases

No	MAX phase	Method of synthesis	Thickness, μm	H, GPa	E, GPa	H/E	Ref.
1	Cr_2AlC	DCMS	6	16	260	0.061	39
2	Cr_2AlC	DCMS	6	19	267	0.071	44
3	Cr_2AlC	DCMS	5…9	12…14	281…283	0.03…0.04	40
4	Cr_2AlC	DCMS	7…9	9…16	223…238	0.02…0.04	38
	Cr_2AlC	MS	6.5	14	212	0.07	100
5	Cr_2AlC	MS	0.5	15	260	0.06	107
6	Cr_2AlC	HiPIMS	3…6	18…20	270…280	0.066…0.071	39
7	Cr_2AlC	HiPIMS	6	14	045	0.056	41
8	Cr_2AlC	CAD/MS	8	13	330	0.039	56
9	Cr_2AlC	CAD/MS	8	17	261	0.065	24
10	$(Cr_{0.76},V_{0.24})_2AlC$	CAD/MS	8	20	315	0.063	24
11	$(Cr_{0.53},V_{0.47})_2AlC$	CAD/MS	8	22	330	0.067	24
12	V_2AlC	CAD/MS	8	23	345	0.067	56
13	V_2AlC	DCMS	4	16	214	0.075	64
14	Ti_2AlC	CAD/MS	8	15	250	0.060	56
15	Ti_3AlC_2	FCAD	2.5	18	240	0.075	26

3.2. EROSION RESISTANCE

Understanding the mechanism of erosion is key to preventing damage and increasing the durability and reliability of materials. Erosion behavior can be significantly influenced by microstructure, hardness, residual stresses, fracture toughness, and long-term stability (e.g., oxidation resistance). A hard substrate can be well protected by a hard coating, while a relatively soft substrate material that plastically deforms under erosion load will result in harmful delamination of the hard coating. When looking for the right combination of coating and substrate, multilayer systems with alternating hard and plastic layers are particularly useful. Such systems are strong enough to prevent particles from penetrating the surface of the materials, yet plastic enough to convert the impact energy of the particles into strain energy [67, 68]. In this regard, MAX phases, due to their specific nanolayer structure, are candidates for achieving this goal.

The review [6] analyzed the results of erosion tests of MAX phase coatings under impact with spherical glass microspheres with an average diameter of 70 μm. An impact particle velocity of 260 m/s at room temperature and an incident angle of 90° were used. A schematic representation of the correlation between HIPMS deposition parameters, structure and erosion mechanism of Cr_2AlC coatings on IN718 substrates is shown in Fig. 3,f–k. The dependence of the structure and morphology of the coatings on the deposition parameters is discussed in more detail in Section 2. The coatings studied had a columnar structure and texture with basal planes (0001) normal to the sample surface (see Fig. 3,a). The erosion mechanisms of the coatings were determined by their density and morphology. Coatings that were denser and finer grained, with strong narrow grain boundaries, exhibited transcrystalline fracture behavior (see Fig. 3,h). The erosion was caused by cohesive delamination parallel to the substrate. The tensile stresses around the impact particle led to the formation of cracks that propagated through the columnar crystals below the surface before turning upward along the base planes, resulting in local damage with the formation of thin flakes (see Fig. 3,j). In contrast, porous and coarse-grained coatings with wide, weak grain boundaries are destroyed in an intercrystalline way (see Fig. 3,i). During particle impact, vertical crack propagation along the columnar crystals to the substrate interface is observed. At the same time, some of the columns are delaminated from the substrate interface and the rest are severely deformed (see Fig. 3,k), indicating low erosion resistance. By using a special heat treatment in vacuum, it was possible to improve the erosion resistance of the coatings, which is related to the phase transformation that occurs during the annealing process. In addition, vacuum annealing resulted in improved adhesion between the coatings and the substrate due to the formation of a mixed diffusion layer and a reduction in compressive internal stresses.

The deposition of a dense Cr_2AlC coating with a thickness of 7 μm on IN718 alloy substrates resulted in a 10-fold reduction in erosion rate and thus a significant increase in erosion resistance compared to the uncoated substrate material. Increasing the thickness of the coating to 20 μm results in about a threefold increase in lifetime [41].

3.3. TRIBOLOGICAL PROPERTIES

Tribological tests of epitaxial films of MAX phases showed a significant dependence of the properties on the load level. For example, for Ti_3SiC_2 (0001) thin films, as the normal load increased from 0.1 mN to 0.24 N, the coefficient of friction μ increased from 0.1 to 0.8 [69]. The high friction and rapid wear under operational loads were attributed to the excessive amount of wear products acting as abrasives. The active formation of hard debris was due to delamination along the base planes due to the weak bond between the MX and A layers. Thus, the (0001) textured film is poorly suitable for wear resistant applications.

The authors of [70] proposed a concept for the design of low-friction coatings using Ti-Al-C as a model system. The self-lubricating friction mechanism was based on a structure consisting of carbide particles in an amorphous carbon matrix. During tribological contact, the amorphous carbon can be graphitized, reducing the coefficient of friction by more than 50% without significant loss of mechanical properties. Paper [6] reports an improvement in tribological properties for polycrystalline textured Cr_2AlC coatings with the base planes (0001) oriented perpendicular to the sample surface. In tests using the 100Cr6 ball/disc scheme at a normal load of 5 N, relatively low wear rates of $2\cdot10^{-6}$ to $6\cdot10^{-6}$ $mm^3\cdot N^{-1}\cdot m^{-1}$ and favorable coefficients of friction μ 0.14…0.4 were obtained, which were further reduced by heat treatment.

In [64], the tribological properties of V-Al-C coatings were investigated in which the MAX phase V_2AlC was formed by annealing amorphous magnetron layers. The tests were carried out at room temperature according to the Al_2O_3 ball/disk scheme at a normal load of 10 N. The average coefficient of friction of the coatings with different MAX phase contents was close to the value of 0.4. The best results were obtained from the coatings annealed at 600 °C, which had the highest hardness and Young's modulus due to the composite structure of nanosized V_2AlC in an amorphous carbon matrix. The lowest friction coefficient of 0.35 resulted in a wear rate of $1.8\cdot10^{-7}$ $mm^3\cdot N^{-1}\cdot m^{-1}$.

Cr_2AlC is considered one of the most promising candidates for medium/high temperature tribological coatings [71–73]. The good tribological properties of this MAX phase are due to the lubricating effect of Cr_2O_3 formed as a result of Cr oxidation at high temperatures [74]; however, one of the main problems in using the Cr_2AlC MAX phase as a protective coating is related to its low hardness in the range of 3.5…5.5 GPa for bulk materials compared to some other MAX phases [75]. Attempts have been made to overcome this problem by producing solid solutions. In [24], a strategy for using a solid solution of V in the M position has been proposed to improve both the mechanical and tribological properties of the Cr_2AlC phase.

Using the combined cathodic arc/magnetron deposition method followed by annealing, coatings of MAX phases of Cr_2AlC and solid solutions of $(Cr_{0.76},V_{0.24})_2AlC$ and $(Cr_{0.53},V_{0.47})_2AlC$ were obtained, the morphology of which is described in Section 2 (see Fig. 3,a–f) [24]. The tribological behavior of the coatings was studied at 900 °C in an atmospheric environment. The tests were carried out according to the Al_2O_3 ball/disk scheme at a normal load of 2 N. During the tests, the Cr_2AlC coating showed an average coefficient of friction of 0.36 and a relatively low wear rate of $7.88\cdot10^{-5}$ $mm^3\cdot N^{-1}\cdot m^{-1}$ due to the formation of a dense oxide double layer on the surface, containing a Cr_2O_3 layer on top and an Al_2O_3 layer in the depth. The position of the layers can be seen in Fig. 3,g, which shows electron microscope images of the cross section of the wear tracks of the coatings after tribological tests. The Cr_2O_3 layer contributed to lubrication and the dense Al_2O_3 layer provided additional protection to the coating by preventing internal oxygen diffusion.

The addition of a small amount of V to the Cr_2AlC coating resulted in a significant decrease in the high-temperature oxidation resistance of the $(Cr_{0.76},V_{0.24})_2AlC$ coating. In solid solution, V atoms occupy the M position of the MAX phase, i.e., V replaces Cr to form bonds with Al and C. However, V is extremely easily oxidized at 900 °C to form V_2O_5, and the M-A and M-X bonds were broken. In this case, the Al and C atoms also bonded with oxygen. Once this process started, the internal diffusion of oxygen was stimulated, causing more severe oxidation of the entire coating. As a result, many pores were formed at the grain boundaries because there was no dense oxide layer on the surface of the coating to provide protection. As a result, the maximum wear rate was obtained for the $(Cr_{0.76},V_{0.24})_2AlC$ coating with a loose structure. However, when the $(Cr_{0.53},V_{0.47})_2AlC$ coating with higher V content was tested, a larger amount of V_2O_5 phase was formed on the surface. The crystalline grains of Al_2O_3 and Cr_2O_3 were surrounded by a large amount of molten V_2O_5, forming a dense structure combining soft and hard phases. During friction, the wear path was continuously filled with liquid lubricant due to the fluidity of the liquid. The $(Cr_{0.53},V_{0.47})_2AlC$ coating had the lowest coefficient of friction of 0.27, which, combined with its high hardness, prevented fracture. The wear track was too small to accurately calculate the wear rate. The amount of molten V_2O_5 was sufficient to form a blocking barrier to external oxygen penetration. The presence of defects on the surface of the coatings in the form of macroparticles of cathode material did not affect the good tribological properties. These results demonstrate that the optimization of the solid solution composition in the coating ensures the production of hard, yet durable, high temperature tribological self-lubricating coatings.

3.4. THE ABILITY FOR SELF-HEALING

In MAX phases, due to the relatively weak M-A bonds between the $M_{n+1}X_n$ layers and the A layers, the A atoms tend to diffuse outward and are easily attacked by oxygen at high temperatures. As a result, the existing microcracks can be filled by the volume expansion caused by the formation of A-based oxides. Therefore, MAX phases are a prime example of self-healing materials [3]. The mechanism of formation of the Al_2O_3 protective scale determines the behavior of these materials during self-healing [76–78]. Typically, the self-healing temperature of Al-based MAX phases is quite high, ranging from 1100 to 1200 °C [76, 77, 79, 80]. An illustrative example of a relatively easy-to-implement strategy for reducing the self-healing temperature of MAX phase based coatings, which consists of partially replacing Al with Sn, is proposed in [81].

A solid solution coating of $Ti_2(Al_{0.6}Sn_{0.4})C$ with the presence of Ti_5Sn_3 (~ 20 wt.%) was prepared by magnetron sputtering and post-thermal treatment. The authors of [81] observed the behavior of cracks caused by the indentation of a Vickers indenter. As shown in Fig. 5,a, quite significant concentric cracks and a small number of radial cracks are formed on the coating surface after indentation. The image in Fig. 5,b shows that the coating surface self-heals by annealing at 700 °C for 10 h, which is significantly less than other results (see Fig. 5,e). The cracks are completely healed and small spherical oxide particles heal the defective areas of the coating. The SEM morphology of the healed crack is shown at different magnifications in Fig. 5,c,d. The dense structure of the formed oxides is visible, while the interface between the coating and the oxides is not completely overgrown, which can be explained by the limited healing time.

A schematic illustration of the self-healing mechanism of the $Ti_2(Al_{0.6}Sn_{0.4})C$ coating is shown in Fig. 5,f. Studies of the distribution of elements and the phase composition of the surface have shown that the formation of SnO_2 oxide is a key factor in realizing crack self-healing at such a low temperature. It has been found that during diffusion in Ti_2AC, the migration energy of Sn (0.66 eV) is lower than that of Al (0.83 eV) [82], which, together with the low melting point of Sn (232 °C), causes a high mobility of Sn atoms in the coating. All this contributes to the preferential movement of Sn to defects with the formation of Sn oxides in an oxidizing atmosphere. In addition, the self-healing $Ti_2(Al_{0.6}Sn_{0.4})C$ coating showed better oxidation resistance at 800 °C in further tests, suggesting a new strategy for the development of protective MAX phases effective at high temperature.

3.5. RESISTANCE TO OXIDATION

It is known that the oxidation resistance of even bulk MAX phases is highly dependent on the characteristics of the substrate, so testing coatings for oxidation at high temperatures in an air atmosphere is highly desirable [7, 83]. It has been shown that MAX phase coatings of the Ti-Al-C and Cr-Al-C systems, like their bulk counterparts, exhibit high oxidation resistance, but a significant influence of substrate material and temperature has been noted. Work [83] studied the oxidation resistance of polycrystalline Ti_2AlN coatings with a thickness of about 10 μm on single crystal Al_2O_3 substrates obtained by sputtering a MAX phase target followed by annealing in vacuum at 800 °C. Cross-sectional studies of Ti_2AlN coatings after oxidation at 900 °C for 1 to 20 h indicate that the thickness of the oxide layer on the surface increases from 0.7 to 2 μm. The oxidation kinetics showed a parabolic behavior with respect to the oxidation time, indicating that the oxidation occurs by oxygen diffusion through the oxide layer. The oxide layer on the surface, mainly composed of Al_2O_3, was continuous and dense, and the oxygen content in the rest of the Ti_2AlN coating was very low. In the diffractograms, α-Al_2O_3 peaks were detected after oxidation for 2 h, while weak TiO_2 peaks were detected only after oxidation for 5 h. That is, the mechanism of the high corrosion resistance of the coatings is explained by the rapid formation of an Al_2O_3 layer on the surface due to the diffusion of more mobile Al atoms in the nanolayer structure of the MAX phases [84]. This mechanism of Al_2O_3 protective scale formation in Al-containing MAX phases is the key mechanism that determines the behavior of these materials during self-healing (Section 3.4).

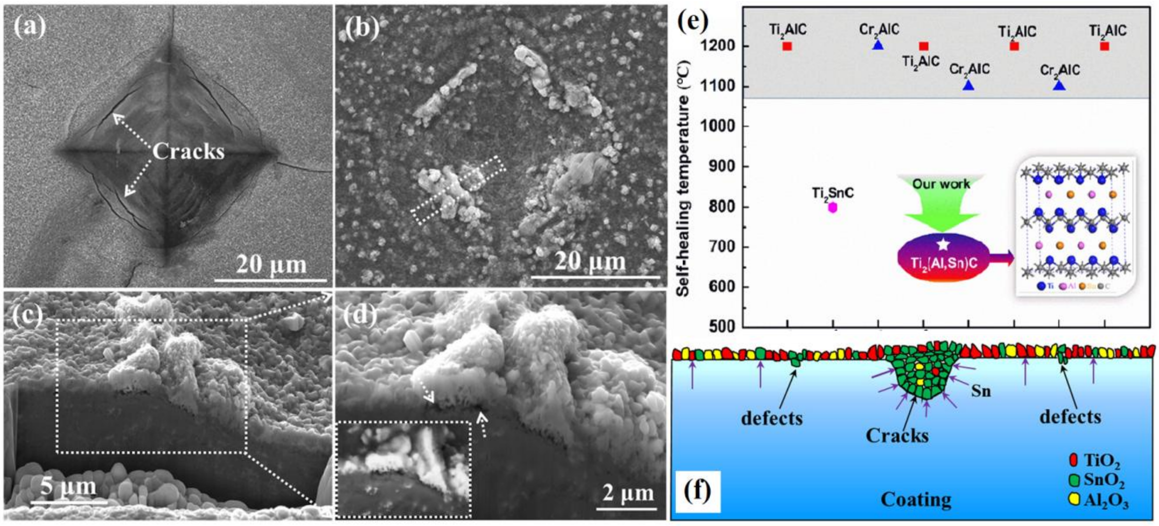

Fig. 5. Surface cracks of $Ti_2(Al_{0.6}Sn_{0.4})C$ coating before self-healing (a). Microstructure of surface cracks after self-healing (b). Enlarged images of self-healing cracks taken from the marked areas (c, d). The results of comparing the self-healing temperatures of different MAX phases (e), Schematic illustration of the self-healing process of $Ti_2(Al_{0.6}Sn_{0.4})C$ coating (f) [81]

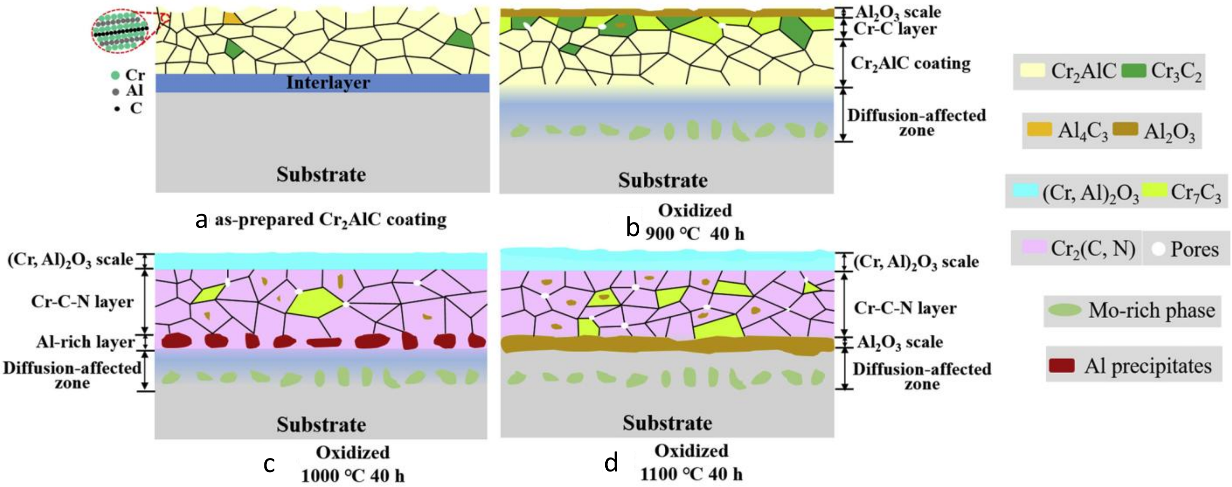

Fig. 6. Schematic diagram of the oxidation mechanism for Cr_2AlC coatings at different temperatures: initial state (a); 900 (b); 1000 (c); 1100 °C (d) [46]

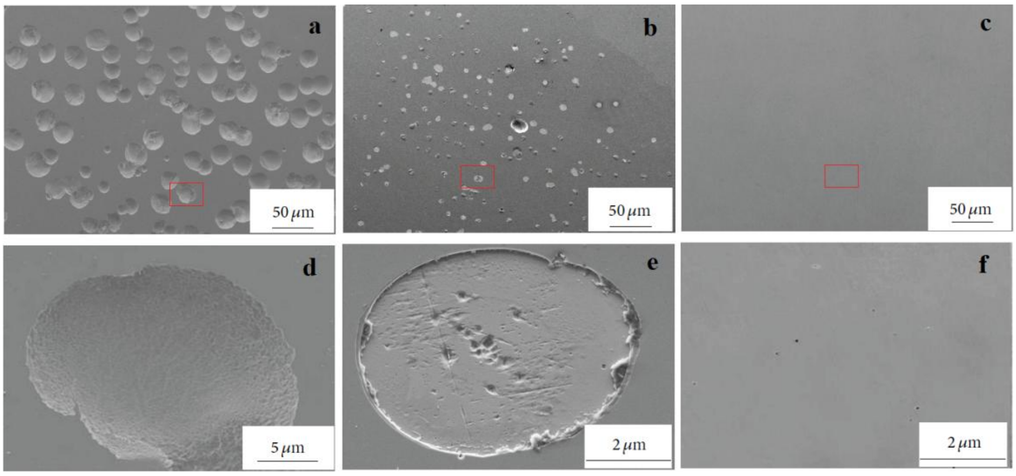

Fig. 7. SEM images of SUS304 substrate (a, d), amorphous Ti-Al-C matrix (b, e), and Ti_2AlC phase MAX coatings (c, f) after corrosion test in 3.5 wt.% aqueous NaCl solution [90]

Similar results were obtained in the study of oxidation of MAX-phase Cr_2AlC coatings on near-α titanium alloy Ti6242 [85]. Tests at 700…800 °C showed an improvement in the oxidation resistance of the coated alloy due to the development of a continuous and dense Al-rich oxide layer, i.e. the Cr_2AlC coating acted as a diffusion barrier for oxygen diffusion inside. The Cr_2AlC coating also improved the oxidation resistance of the nickel-based M38G superalloy at 900…1100 °C, although the observed oxidation rate was about an order of magnitude higher than the corresponding oxidation rate of the bulk MAX phase [86]. On the contrary, in works [87, 88], the oxidation resistance of composite vacuum-arc coatings with the MAX phase Ti_2AlC was higher than the resistance of the bulk material. Coatings with a thickness of 6 μm on Ti foil substrates were annealed in air at a temperature of 600 °C for 1000 h. The average rate of mass gain for the coatings was $(6…7)\cdot10^{-5}$ $mg\cdot cm^{-2}\cdot h^{-1}$, which was 2 times less than for the Ti_2AlC-based cathode material and an order of magnitude less than for the Ti substrate.

For Cr_2AlC coatings, it has been shown that oxidation resistance can be improved by changing the coating morphology from columnar to equilibrium, since columnar coatings oxidize rapidly due to the increased diffusion of oxygen into the coating along the grain boundaries [38, 89]. In addition to morphology, the phase purity of coatings is important during oxidation as it also affects the rate of migration of aluminum atoms. In [90] it was shown that the Ti_2AlC phase MAX films have a better oxidation resistance compared to the amorphous Ti-Al-C initial films, since they are characterized by a lower mass gain rate and a thinner oxide layer.

An important characteristic of protective coatings is their resistance to oxidation in a high-temperature steam atmosphere. In [91], the oxidation resistance in pure steam at 1000…1200 °C of a 12-μm thick Ti_2AlC coating deposited on Zirlo alloy by a combined cathodic arc/magnetron method followed by vacuum annealing was investigated. The oxidation resistance of the Zirlo substrate was significantly improved by the coating with a dense columnar-free microstructure due to the formation of a triple oxide scale α-Al_2O_3+TiO_2(rutile)/α-Al_2O_3/TiO_2. A thinner but single phase and dense magnetron deposited Ti_2AlC coating of 5 μm thickness on a Zircaloy-4 substrate also shows high resistance to oxidation in steam at 800 °C. The oxide film was a multilayer structure with a metastable θ-Al_2O_3-rich layer on the surface. However, rapid oxidation at 1000 °C resulted in cracking and delamination of the coatings [92].

One of the limiting factors for the use of MAX phases as protective coatings on metal substrates is the insufficient thermal stability of this interface. In particular, the diffusion of Al from the MAX phase into a metal substrate such as stainless steel [93], Ti alloy with Al [43], Ni-based superalloy [94, 95], or Zr alloy [92, 96]. In [43], coatings of Ti-Al-C and Cr-Al-C systems with thicknesses greater than 7 μm were deposited on TiAl48-2-2 alloy by magnetron sputtering. The MAX phases of Ti_3AlC_2, Ti_2AlC or Cr_2AlC were formed in the coatings as a result of annealing in air with simultaneous development of protective oxide layers, which replaced the traditional additional post-thermal treatment in an inert atmosphere. The oxidation resistance of the MAX phases was investigated by long annealing at 800…850 °C. The Ti_3AlC_2 and Ti_2AlC phases on alumina or TiAl48-2-2 alloy substrates showed high thermodynamic stability and excellent oxidation resistance due to the formation of slowly growing protective oxide layers. For the Ti_2AlC coatings, excellent oxidation behavior on the alloy was confirmed during 300 h of exposure at 850 °C. However, the MAX phase of Cr_2AlC on the TiAl48-2-2 alloy proved to be thermodynamically unstable. The Cr_2AlC coating is destroyed after 100 h at 800 °C due to mutual diffusion between the coating and the substrate and the concomitant transformation of the MAX phase into carbides and nitrides.

The mechanism of oxidation of Cr_2AlC coatings at different temperatures in the range of 900…1100 °C has been studied in detail in [46]. The oxidation behavior of MAX phase Cr_2AlC coatings (purity 91 wt.%) with a thickness of ~ 10 μm on Hastelloy alloy substrates, obtained by a combined cathodic arc/magnetron method followed by vacuum annealing, was studied. The coatings exhibited a dense, columnar structure similar to that shown in Fig. 3. The oxidation of Cr_2AlC coatings was studied for 40 h at different temperatures in the range of 900…1100 °C. It was found that the oxidation kinetics followed a parabolic law at each temperature. With an increase in temperature from 900 to 1100 °C, the average rate of increase in mass of the coatings increased approximately 5-fold from $6.3\cdot10^{-3}$ to $3.7\cdot10^{-2}$ $mg\cdot cm^{-2}\cdot h^{-1}$. A similar parabolic dependence of mass increase on oxidation time is characteristic of MAX phase coatings of various systems [97–99].

A schematic diagram of the oxidation mechanism for Cr_2AlC coatings at different temperatures is shown in Fig. 6. At 900 °C, a continuous surface layer of Al_2O_3 was obtained due to the selectivity of the oxidation. In the near-surface layer, this resulted in the deficiency of Al in the MAX phase and the transformation of Cr_2AlC into Cr_7C_3 and Cr_3C_2 phases, but most of the coating retained the structure of the MAX phase. When the annealing temperature was increased to 1000…1100 °C, a mixed oxide layer consisting of Cr_2O_3 and Al_2O_3 was identified on the surface, and the MAX phase in the coating decomposed due to the diffusion of Al into the substrate to form Cr_7C_3 and $Cr_2(C,N)$. At 1100 °C, the Al-enriched layer at the coating/substrate interface transforms into dense α-Al_2O_3, which serves as a barrier to substrate oxidation. Although the results showed a strong dependence of oxidation on temperature, the coated samples remained intact even after oxidation at 1100 °C. Thus, despite the diffusion of Al into the substrate and the instability of the MAX phase, the Cr_2AlC coating shows good protection of the nickel alloy against oxidation.

To inhibit the diffusion of Al into a metal substrate and to stabilize the MAX phase, the deposition of a metal or ceramic layer between the substrate and the coating, which acts as a diffusion barrier, has been successfully used. In [84], a double barrier layer consisting of ZrN and AlN with a total thickness of ~2 μm was deposited between a Cr_2AlC magnetron coating and a Zr substrate. To protect against high temperature oxidation in steam, a 0.5 μm thick TiC layer was deposited between the Zr alloy and the Ti_2AlC magnetron coating [92]. For HiPIMS coatings of Cr_2AlC on TiBw/Ti6Al4V composite substrates, a ~ 1 μm thick Ti layer successfully performed as a diffusion barrier [39]. In [45], a diffusion layer of $Ti_{29}Al_{25}N_{46}$ with the same thickness was used for IN718 and WC-Co substrates, and in [24], a Cr layer with a thickness of ~ 350 nm was used.

In [100], a 0.5 μm thick Cr buffer layer was applied between the Zircaloy-4 alloy and the Cr/C/Al magnetron multilayer coating, which successfully prevented Al diffusion into the substrate during high-temperature tests, but failed to prevent the formation of microcracks on the surface of the 6.5 μm thick coating due to annealing at 550 °C, which was used to form the MAX phase of Cr_2AlC. The appearance of cracks was caused by a large difference in the coefficient of thermal expansion between Cr_2AlC and Zircaloy, which limits the ability to use the coating for ATF. These microcracks can lead to early coating failure under normal reactor conditions [101]. In addition, the annealing temperature of 550 °C is slightly higher than the typical stress relief annealing (SRA) temperature for zirconium alloy tubes (~ 400 °C) according to current industrial manufacturing processes. The authors of [100] proposed the use of an alternative coating annealed at a lower temperature of 400 °C, which had no cracks, but this temperature was not sufficient for the formation of the MAX phase, so the nanocomposite structure of the coating consisted of binary carbides and intermetallic phases. Interestingly, the coatings annealed at 400 and 550 °C had the same oxidation mechanisms and significantly improved the resistance to high-temperature oxidation of Zircaloy-4 alloy in tests from 300 to 1000 °C coupled with a subsequent holding time of 10 min at 1000 °C. This is due to the transformation of the coating structure, which did not contain the MAX phase, into Cr_2AlC during the heating period (phase transformation temperature ~ 480 °C). Thermal shock tests showed that the coatings have high adhesion and microcracks can self-heal at high temperature due to the formation of alumina. Autoclave tests at 330 °C and 18 MPa for 30 days showed that the coating annealed at 400 °C has excellent resistance to hydrothermal corrosion due to the thin passivation layer of Cr_2O_3. Therefore, annealing the coating at 400 instead of 550 °C is a reasonable solution to avoid cracking of the MAX phase coating and maintain its excellent resistance.

3.6. CORROSION RESISTANCE

The ability of MAX phases to form dense and stable passivation films on the surface in various environments makes it possible to produce coatings with excellent corrosion resistance based on them. Table 2 shows the results of the analysis of potential-dynamic polarization curves of PVD samples coated with some MAX phases. For comparison, the values of corrosion potential (E_{corr}) and corrosion current density (I_{corr}) for uncoated stainless steel substrates and coated substrates are shown. In general, the higher the E_{corr} and the lower the I_{corr}, the better the corrosion resistance of the material. Table 2 shows that I_{corr} decreased significantly after the deposition of the coating, i.e. the substrate was effectively protected from the corrosive environment [26].

In [90], the corrosion properties of HiPIMS coatings of Ti-Al-C deposited on a SUS304 substrate were investigated. The MAX phase of Ti_2AlC was formed in the coating by annealing the amorphous coating formed after deposition. Corrosion tests were performed at room temperature in a 3.5 wt.% aqueous NaCl solution simulating a marine corrosive environment. The values of E_{corr} and I_{corr} for the MAX phase of Ti_2AlC were –0.301 V and $5.82 \cdot 10^{-8}$ A·cm^{-2}, respectively. The amorphous coated sample had slightly lower values of –0.618 V and $1.44 \cdot 10^{-8}$ A·cm^{-2}, although better than the substrate. Fig. 7 shows SEM images of the surface of the samples after testing. Significant corrosion damage with a large number of defects can be observed on the surface of the uncoated SUS304 substrate (see Fig. 7,a,d). The surface of the sample with amorphous Ti-Al-C coating looks slightly better (see Fig. 7,b,e). However, there are no obvious punctures and pores on the surface of the MAX phase. Thus, the Ti_2AlC MAX phase coating provides more effective protection than an amorphous coating of similar composition, which correlates with the results of the oxidation resistance tests (see Section 3.5).

The above conclusion is in agreement with the results of [26], where FCVA coatings based on the MAX phase of Ti_3AlC_2 were studied, for the formation of which annealing at different temperatures from 600 to 1000 °C was used. The annealing temperature significantly affected the phase composition and crystallinity of the coatings. As the temperature increased, the structure changed from a low crystalline mixture of Ti_3AlC_2 and Ti_xAl_y to a predominant content of the TiC phase. As a result, the corrosion resistance of the coatings in an aqueous NaCl solution first increased and then decreased with increasing annealing temperature. The coating annealed at 800 °C showed the best corrosion resistance due to the dominance of the Ti_3AlC_2 phase.

MAX phase coatings are being considered as a protective coating material for metal bipolar plates of Proton Exchange Membrane Fuel Cells (PEMFCs) operating in humid, acidic and high temperature environments. Corrosion tests in a solution of 0.5 M H_2SO_4 + (2…5) ppm F^- at 70…80 °C model the PEMFC environment. The MAX coatings of Ti_3SiC_2 [102], Ti_3AlC_2 [103], and Cr_2AlC [62] phases deposited on stainless steel substrates by magnetron or combined methods followed by vacuum annealing show good corrosion characteristics with low corrosion current density (see Table 2). The mechanism underlying the high corrosion resistance of MAX phases in an aggressive environment is explained by the formation of an oxide layer on the surface of the sample. The high corrosion resistance of the bulk MAX phase of Ti_3SiC_2 in H_2SO_4 and HCl is attributed to the fact that Ti atoms on the surface are leached and Si atoms are oxidized to form a protective layer based on SiO_2. The study of the corrosion behavior of the Ti_3AlC_2 phase showed good corrosion resistance in NaOH due to the formation of a dense and stable passivating TiO_2 film. However, the corrosion resistance of Ti_3AlC_2 in H_2SO_4 was worse, which is explained by the formation of sub-stoichiometric metastable TiO_{2-x} [22]. Nevertheless, all considered coatings significantly improved the corrosion resistance of stainless steel substrates in the PEMFC model environment and their I_{corr} values met the technical requirements ($< 10^{-6}$ A cm^{-2}) for bipolar plates [62]. Intermediate layers of Ti and TiC for Ti-containing MAX phases or Cr_3C_7 for Cr_2AlC were used to achieve better adhesion between the substrate and the coatings and to reduce the stresses occurring between the substrate and the coatings. The best corrosion resistance with I_{corr} $2 \cdot 10^{-8}$ A·cm^{-2} was shown by the Cr_2AlC coating with a 2.3 μm thick Cr_3C_7 sublayer, which was responsible for the formation of the preferred orientation (103) of the MAX phase [62].

Table 2

Analysis of corrosion parameters of uncoated steel substrates and substrates with MAX phase coatings from potential dynamic polarization curves data

No	Sample Description	Method of coating deposition	Test environment	Test temperature, °C	E_{corr}, V	I_{corr}, A·cm^{-2}	Ref.
1	Substrate SUS304	HiPIMS	3.5 wt.% NaCl solution	KT	-0.529	$1.91 \cdot 10^{-5}$	90
	Coating Ti_2AlC				-0.301	$5.82 \cdot 10^{-8}$	
2	Substrate SUS304	FCAD		KT	-0.511	$9.73 \cdot 10^{-8}$	26
	Coating Ti_3AlC_2				-0.325	$5.63 \cdot 10^{-9}$	
3	Substrate SS304	MS	0.5 M H_2SO_4 + (2…5) ppm F^-	70	-0.380	$2.98 \cdot 10^{-4}$	103
	Coating Ti_3AlC_2 (sublayer Ti/TiC)				–	$4.4 \cdot 10^{-7}$	
4	Substrate SS304	MS		70	-0.380	$2.98 \cdot 10^{-4}$	102
	Coating Ti_3SiC_2 (sublayer Ti)				0.129	$7.38 \cdot 10^{-7}$	
5	Substrate SS316L	CAD/MS		80	-0.120	$5 \cdot 10^{-5}$	62
	Coating Cr_2AlC (sublayer Cr_3C_7)				0.125	$2 \cdot 10^{-8}$	

3.7. RADIATION RESISTANCE AND HYDROGEN PERMEABILITY

MAX phase films can be used as protective coatings for fuel rod cladding and structural materials of nuclear reactors; however, far fewer results on radiation resistance have been obtained for MAX phases in the form of coatings compared to bulk materials. Currently, most studies of the radiation resistance of MAX phase coatings focus on the study of Cr_2AlC and Ti_2AlC coatings, particularly as a material for protective layers for ATF cladding [12, 28, 104]. In radiation materials science, the intensity of radiation defect generation is usually characterized by the number of atomic displacements in a given time (dpa). For most modern reactors (WWER, PWR, BWR), this value is in the range of 0.05 to 60 dpa for 40 years. For fast reactor cores and advanced reactor models, this value can reach 100…200 dpa/year. The most adequate reproduction of real conditions in a nuclear reactor can be achieved by "hot implantation" of heavy ions, but a first approximation can be achieved by irradiation at room temperature with post-implantation annealing [105].

The effect of 320 keV heavy Xe^{2+} ion irradiation on Cr_2AlC and Cr_2GeC epitaxial films grown on Al_2O_3 (0001) substrates at 800 °C by the magnetron sputtering method has been studied in situ by electron microscopy. Both compounds amorphize at moderate doses ($10^{13}…10^{14}$ ions·cm^{-2}), but exhibit different amorphization mechanisms, indicating a significant influence of the chemical composition of the MAX phase on the process. It is suggested that amorphization in Cr_2GeC occurs by a direct impact process, while in Cr_2AlC it is determined by the defect accumulation process, which determines the excellent tolerance of the latter. The MAX phase of Cr_2AlC at 2.2 dpa amorphized partially due to the transformation into the intermediate phase $(Cr,Al)_2C_x$ (known as the γ phase), which eventually leads to the amorphous state. Complete amorphization was observed at 6.2 dpa when irradiated at room temperature [106].

Cr_2AlC nanocrystalline coatings with a thickness of ~ 1 μm, obtained by magnetron sputtering followed by annealing at a lower temperature of about 600 °C, showed slightly worse resistance to irradiation with Xe^+ ions with an energy of 320 keV at room temperature. At 300 K, the Cr_2AlC phase started to amorphize at a displacement level of about 0.3 dpa. Above 3.3 dpa, the entire crystal structure was almost completely lost. In contrast, irradiation at 623 K (350 °C) did not show amorphization up to 90 dpa, which is attributed to the nanocrystalline nature of the MAX phase, which prevents transformation to the γ-phase, the presence of many grain boundaries, and the low energy barrier to defect recombination [107]. Later, it was shown that an increase in phase stability up to 138 dpa was achieved by varying the ideal stoichiometry of the MAX phase, leading to the formation of a two-phase nanocrystalline structure based on Cr_2AlC together with Cr_5Al_8 in $Cr_2Al_{0.75}C$ coatings [108].

The study of the effect of the second phase on the mechanisms of radiation resistance was continued in [109]. The two-phase Cr_2AlC material was deposited by magnetron sputtering at a temperature as low as 375 °C. The coating contains a stoichiometric columnar nanocrystalline matrix of the MAX phase, as well as amorphous spherical nanoparticles of the same composition as the second phase. At a maximum dose of 40 dpa, which extrapolates the environment of future nuclear fusion reactors [105], no complete amorphization of the two-phase coating was observed. It is assumed that the amorphous nanophase, due to its larger free volume, helps to reduce the accumulation of displacement defects in the MAX phase, thus preventing its amorphization. A link between the nucleation and growth of inert gas bubbles and radiation-induced Cr segregation along grain boundaries was found. Surprisingly, the results suggest that amorphous nanoparticles may be useful for the Cr_2AlC MAX phase under extreme irradiation conditions, which unexpectedly contradicts traditional ideas about ceramics [109].

One of the primary sources of material degradation in nuclear reactors is the formation of transmutation reaction products such as hydrogen and helium. The resulting atoms change the macroscopic properties of the irradiated material and contribute to helium embrittlement, hydrogen embrittlement and gas swelling. Implantation of hydrogen and helium into the reactor material with a dose greater than $1{\cdot}10^{16}$ ions·cm^{-2} effectively simulates the process of actual operation [105]. Work [110] investigated radiation damage to polycrystalline Cr_2AlC films deposited on Al_2O_3 (0001) substrates by the method of RF reactive magnetron sputtering. The films were irradiated with He^+ ions at 100 keV with a dose range of $5{\cdot}10^{15}$ to $1{\cdot}10^{17}$ ions·cm^{-2} at room temperature. It is shown that the Cr_2AlC film is sensitive to irradiation at a damage level of 1.16 dpa. A dose of $1{\cdot}10^{17}$ ions·cm^{-2} causes severe damage to the arrangement of MAX phase atoms, which transforms into a disordered solid solution of $(Cr,Al)_2C_x$. At the same time, modeling of the damage depth profile in the Cr_2AlC film using the SRIM-2013 code showed a maximum at a depth of 384 nm with a value of 5.4 dpa and a maximum ion travel profile at 430 nm. However, the irradiation-induced structural damage in Cr_2AlC is significantly recovered by thermal annealing at temperatures around 600 °C, which is attributed to the high diffusion of defects. The damaged phase $(Cr,Al)_2C_x$ completely disappeared, and polycrystalline Cr_2AlC was recovered. Al atoms play an important role in repairing radiation damage due to the low formation energy of cationic antistructural defects. After annealing at 750 °C, the hardness of the irradiated films was almost completely recovered, which is explained by both the recombination of defects and the repair of damaged chemical bonds. When the annealing temperature is lower than 600 °C, most of the implanted He atoms still remain in the Cr_2AlC film. The significant release of He with the formation of bubbles and blisters with a diameter of 5…7 μm on the surface, which occurs at an annealing temperature of 750 °C, is closely related to the repair of damage [111].

A similar reversible phase transformation was also found in Ti_2AlC magnetron polycrystalline films. The phase transformation from hcc-Ti_2AlC to fcc-$(Ti_2Al)C$ occurred during irradiation with He^+ ions at an energy of 110 keV, while the reversible phase transformation from fcc-$(Ti_2Al)C$ to hcc-Ti_2AlC occurred during post-annealing at temperatures above 600 °C [112]. Thus, the reversible phase transformation of MAX phase coatings indicates the dynamic reduction of this material and provides insight into the design of new irradiation resistant ceramic materials.

The penetration of hydrogen through the protective layer is an important parameter for the safety of the base material. Based on DFT calculations for the Cr_2AlC phase, it was found that due to the weak M-A bond in the MAX phase, H atoms tend to diffuse parallel to the Al plane [113], which means that in the presence of texture in the coating, the orientation of the base plane (0001) parallel to the substrate surface is more favorable. In fact, the MAX magnetron coatings of Ti_2AlC and Cr_2AlC phases with a texture (0001) applied to the surface of Zircaloy-4 effectively suppress hydrogen absorption. Coatings with a thickness of 5 μm MAX are as effective as a 30 μm pre-oxidized ZrO_2 layer, which reduces hydrogen penetration below the detection limit [114]. In [93], Ti_2AlN coatings with a texture (0001) of ~ 3 μm thickness on an AISI 430 steel substrate showed high permeation reduction factors (PRF). At a temperature of 300 °C, the PRF was 45. However, the formation of oxide scale during annealing of the coating on the substrate for 2 h at a temperature of 700 °C leads to a further decrease in permeation. Due to the formation of an 80 nm thick oxide layer on the coating surface, a PRF value of approximately 3700 was achieved. Such a significant decrease in penetration can be explained by the low solubility of hydrogen in the α-Al_2O_3 phase as well as the potential healing of small defects in Ti_2AlN, blocking alternative migration pathways with low energy barriers.

CONCLUSIONS

The unique hybrid properties of ceramics and metals due to their special nanolayer structure make $M_{(n+1)}AX_n$ phases an attractive material for important structural components operating in extreme environments. Successes in the development of PVD processes for the synthesis of nanocrystalline coatings of MAX phases up to 10 μm thick at low temperatures on technologically important substrates open up significant prospects for the creation of multifunctional coatings that are resistant to high temperature, oxidation, corrosion, deformation, wear, and irradiation. Such coatings can be effectively used to provide comprehensive protection for titanium, aluminum, zirconium alloys, steels, and nickel-based superalloys operating under severe high-temperature, corrosive, and radiation conditions that are important to the aerospace, automotive, marine, chemical, and nuclear power industries.

The most studied MAX phases in PVD coatings include Ti_2AlC, Ti_3AlC_2, Ti_3SiC_2, V_2AlC, but the predominant interest in Cr_2AlC remains undisputed. The Cr_2AlC phase attracts much attention because of its excellent resistance to high temperature oxidation and hot corrosion due to the formation of continuous, dense and thermodynamically stable oxide layers.

Various types of magnetron sputtering, including in combination with cathodic arc deposition, are commonly used to deposit PVD coatings of MAX phases. The general relationships between PVD deposition parameters and structural properties of MAX phase coatings are similar to those known for other nanostructured metal carbides and nitrides. The substrate temperature and the energy of the particles forming the coating have a decisive influence on their composition, morphology, surface roughness, texture, crystallite size and stress, even when the MAX phase is formed in a two-step process by annealing a coating with an intermediate, usually amorphous, structure. MAX phase PVD coatings have now been synthesized and show high protective properties. Further tuning of the performance of MAX phases depends largely on solid solution approaches, where the complexity of the composition allows further improvement of the properties.

Research results show that the protective properties of MAX phase coatings with an equilibrium structure, which can be obtained by a two-step process, are often higher than columnar coatings in which the MAX phase is formed during deposition.

The most attractive is their ability to improve the protective properties at high temperatures (500…800 °C), in particular due to the mechanisms of self-lubrication or self-healing of damages of mechanical or radiation origin. In addition to the main MAX phase, high quality PVD coatings often contain a small amount of amorphous or carbide/nitride phases, which affects their properties. Sometimes this effect can be positive, particularly in terms of tribological properties or radiation resistance. Under certain conditions, phase transformations caused by decomposition of the MAX phase at temperatures above 1000…1100 °C do not cause coating destruction and catastrophic degradation of protective properties.

Nevertheless, the analysis of literature data shows that research is needed in many areas before MAX phase coatings can be confidently transferred to the market. Identifying the relationships between PVD deposition parameters, structure and properties of MAX phase coatings remains an urgent need for the introduction of these materials in various fields.

ACKNOWLEDGEMENTS

The work was financially supported by the National Academy of Science of Ukraine (program “Support of the development of main lines of scientific investigations” (KPKVK 6541230)).

REFERENCES

1. M. Dahlqvist, M.W. Barsoum, J. Rosen. MAX phases – Past, present, and future // *Materials Today*. 2024, 72, p. 1-24.
2. J. Gonzalez-Julian. Processing of MAX phases: From synthesis to applications // *J. Am. Ceram. Soc.* 2021, v. 104, p. 659-690.
3. Z. Zhang, X. Duan, D. Jia, Y. Zhou, S. Van Der Zwaag. On the formation mechanisms and properties of MAX phases: A review // *J. Eur. Ceram. Soc.* 2021, v. 41, p. 3851-3878.
4. M.W. Barsoum, T. El-Raghy. The MAX phases: Unique New Carbide and Nitride Materials // *American Scientist.* 2001, v. 89, p. 334-343.
5. P. Eklund, M. Beckers, U. Jansson, H. Högberg, L. Hultman. The $M_{n+1}AX_n$ phases: Materials science and thin-film processing // *Thin Solid Films*. 2010, v. 518, N 8, p.1851-1878.
6. O. Berger. The correlation between structure, multifunctional properties and application of PVD MAX phase coatings. Part I. Texture and room temperature properties // *Surface Engineering*. 2020, v. 36, N 3, p. 225-267.
7. O. Berger. The correlation between structure, multifunctional properties and applications of PVD MAX phase coatings. Part II. Texture and high-temperature properties // *Surface Engineering*. 2020, v. 36, N 3, p. 268-302.
8. O. Berger. The correlation between structure, multifunctional properties and application of PVD MAX phase coatings. Part III. Multifunctional applications. Surface Engineering // *Surface Engineering*. 2020, v. 36, N 3, p. 303-325.
9. A. Biswas, V. Natu, A.B. Puthirath. Thin film growth of MAX phases as functional materials // *Oxford Open Materials Science.* 2021, v. 1, N 1, itab020.
10. E.N. Reshetnyak, A.S. Kuprin, M.A. Bortnitskaya, T.A. Prikhna, V.A. Belous. Synthesis, structure and protective properties of PVD MAX phase coatings. A review. Part I. MAX phase coatings deposition // *Problems of Atomic Science and Technology*. 2023, N 5(147), p. 111-125.
11. Z.M. Sun. Progress in research and development on MAX phases: a family of layered ternary compounds // *International Materials Reviews*. 2011, v. 56, N 3, p. 143-166.
12. C. Wang, C.L. Tracy, R.C. Ewing. Radiation effects in $M_{n+1}AX_n$ phases featured // *Appl. Phys. Rev.* 2020, v. 7, N 4, p. 041311.
13. M.W. Barsoum, M. Radovic. Elastic and Mechanical Properties of the MAX Phases // *Annu. Rev. Mater. Res.* 2011, v. 41, p. 195-227.
14. J.C. Nappé, P. Grosseau, F. Audubert, B. Guilhot, M. Beauvy, M. Benabdesselam, et al. Damages induced by heavy ions in titanium silicon carbide: Effects of nuclear and electronic interactions at room temperature // *J. Nucl. Mater.* 2009, v. 385, N 2, p. 304-307.
15. D. Bowden, J. Ward, S. Middleburgh, S.S. de Moraes, E. Zapata-Solvas, T. Lapauw, et al. The stability of irradiation-induced defects in Zr_3AlC_2, Nb_4AlC_3 and $(Zr_{0.5}, Ti_{0.5})_3AlC_2$ MAX phase-based ceramics // *Acta Mater.* 2020, v. 183, p. 24-35.
16. D.R. Hussein, K.K. Abbas, A.M.H. Al-Ghaban. Overview of structural, electronic, elastic, thermal, optical, and nuclear properties of Zr_2AC (A=Al, Si, P, S, Ge, As, Se In, Sn, Tl, and Pb) MAX phases: A brief review // *Heliyon*. 2023, v. 9, N 8, e18303.
17. J. Gonzalez-Julian, G. Mauer, D. Sebold, D.E. Mack, R. Vassen. Cr_2AlC MAX phase as bond coat for thermal barrier coatings: Processing, testing under thermal gradient loading, and future challenges // *Journal of the American Ceramic Society.* 2020, v. 103, N 4, p. 2362-2375.
18. C. Azina, S. Mráz, M. Hans, D. Primetzhofer, J.M. Schneider, P. Eklund. Oxidation behaviour of V_2AlC MAX phase coatings // *J. Eur. Ceram. Soc.* 2020, v. 40, N 13, p. 4436-4444.
19. I. Salama, T. El-Raghy, M.W. Barsoum. Oxidation of Nb_2AlC and $(Ti, Nb)_2AlC$ in air // *J. Electrochem. Soc.* 2003, v. 150, N 3, p. 152-158.

20. Y. Du, J.X. Liu, Y. Gu, X.G. Wang, F. Xu, G.J. Zhang. Anisotropic corrosion of Ti_2AlC and Ti_3AlC_2 in supercritical water at 500 ºC // *Ceramics International*. 2017, v. 43, N 9, p. 7166-7171.

21. Z. Zhang, Y. Qian, J. Xu, J. Zuo, M. Li. Effect of annealing on microstructure evolution and corrosion resistance of an amorphous Cr-Al-C coating // *Corrosion Science*. 2021, v. 178, p. 10906.

22. D. Li, Y. Liang, X. Liu, Y. Zhou. Corrosion behavior of Ti_3AlC_2 in NaOH and H_2SO_4 // *Journal of the European Ceramic Society*. 2010, v. 30, N 15, p. 3227-3234.

23. W. Tian, P. Wang, Y. Kan, G. Zhang. Oxidation behavior of Cr_2AlC ceramics at 1100 and 1250 °C// *J. Mater. Sci.* 2008, v. 43, p. 2785-2791.

24. Z. Wang, C. Wang, Y. Zhang, A. Wang, P. Ke. M-site solid solution of vanadium enables the promising mechanical and high-temperature tribological properties of Cr_2AlC coating // *Materials and Design*. 2022, v. 222, p. 111060.

25. Z. Tian, P. Zhang, W. Sun, B. Yan, Z. Sun. Vegard's law deviating $Ti_2(Sn_xAl_{1-x})C$ solid solution with enhanced properties // *Journal of Advanced Ceramics.* 2023, v. 12(8), p. 1655-1669.

26. H. Li, H. Cao, J. Yang, Y. Li, F. Qi, N. Zhao, X. Ouyang. Influence of annealing temperature on the structure and properties of Ti_3AlC_2 coatings by FCVA method // *Materials Characterization*. 2022, v. 194, p. 112421.

27. A. Loganathan, A. Sahu, C. Rudolf, C. Zhang, S. Rengifo, T. Laha, B. Boesl, A. Agarwal. Multi-scale tribological and nanomechanical behavior of cold sprayed Ti_2AlC MAX phase coating // *Surface and Coatings Technology.* 2018, v. 334, p. 384-393.

28. B. Garcia-Diaz, L. Olson, C. Verst, R. Sindelar, E. Hoffman, B. Hauch, B. Maier, K. Sridharan. MAX phase coatings for accident tolerant nuclear fuel // *Trans. Am. Nucl. Soc.* 2014, v. 110, p. 994-996.

29. Y.P. Chien, S. Mráz, C. Azina, S. Kolozsvári, P. Polcik, J.M. Schneider. Stoichiometric Cr_2AlC MAX phase as bond coat for thermal barrier coatings phase coatings deposited by HPPMS from composite targets using industrial deposition technology // *Open Ceramics*. 2024, v. 17, p. 100538.

30. Z. Mahmoudi, S.H. Tabaian, H.R. Rezaie, F. Mahboubi, M.J. Ghazali. Synthesis of Ti_2AlC and Ti_3AlC_2 MAX phases by arc-PVD using Ti–Al target in C_2H_2/Ar gas mixture and subsequent annealing // *Ceram. Int.* 2020, v. 46, N 4, p. 4968-4975.

31. Z. Feng, P. Ke, A. Wang. Preparation of Ti_2AlC MAX Phase Coating by DC Magnetron Sputtering Deposition and Vacuum Heat Treatment // *J. Mater. Sci. Technol*. 2015, v. 31, p. 1193-1197.

32. M. Orhing. *Materials Science of Thin Films: Deposition and Structure.* London: Academic Press, 2001, 794 p.

33. D. Manova, J.W. Gerlach, S. Mandl. Thin Film Deposition Using Energetic Ions // *Materials*. 2010, v. 3, p. 4109-4141.

34. O. Wilhelmsson, J.P. Palmquist, T. Nyberg, U. Jansson. Deposition of Ti_2AlC and Ti_3AlC_2 epitaxial films by magnetron sputtering // *Appl. Phys. Lett*. 2004, v. 85, p. 1066.

35. O. Wilhelmsson, J.P. Palmquist, E. Lewin, J. Emmerlich, P. Eklund, P.O. Å. Persson, H. Högberg, S. Li, R. Ahuja, O. Eriksson, L. Hultman, U. Jansson. Deposition and characterization of ternary thin films within the Ti–Al–C system by DC magnetron sputtering // *J. Cryst. Growth*. 2006, v. 291, p. 290.

36. M.C. Guenette, M.D. Tucker, M. Ionescu, M. Bilek, D.R. McKenzie. Cathodic arc co-deposition of highly oriented hexagonal Ti and Ti_2AlC MAX phase thin films // *Thin Solid Films*. 2010, v. 519, N 2, p. 766-769.

37. Z. Zhang, H. Jin, J. Chai, J. Pan, H.L. Seng, G.T.W. Goh, L.M. Wong, M.B. Sullivan, S.J. Wang. Temperature-dependent microstructural evolution of Ti_2AlN thin films deposited by reactive magnetron sputtering // *Applied Surface Science.* 2016, v. 368, p. 88-96.

38. A. Obrosov, R. Gulyaev, A. Zak, M. Ratzke, M. Naveed, W. Dudzinski, S. Weiß. Chemical and Morphological Characterization of Magnetron Sputtered at Different Bias Voltages Cr-Al-C Coatings // *Materials*. 2017, v. 10, N 2, p. 156 (16).

39. M.W. Qureshi, X. Ma, G. Tang, B. Miao, J. Niu. Fabrication and Mechanical Properties of Cr_2AlC MAX Phase Coatings on TiBw/Ti_6Al_4V Composite Prepared by HiPIMS // *Materials*. 2021, v. 14, N 4, p. 826.

40. M. Naveed, A. Obrosov, A. Zak, W. Dudzinski, A.A. Volinsky, S. Weiß. Sputtering Power Effects on Growth and Mechanical Properties of Cr_2AlC MAX Phase Coatings // *Metals.* 2016, v. 6, N 11, p. 265 (11).

41. D. Eichner, A. Schlieter, C. Leyens, L. Shang, S. Shayestehaminzadeh, J. M. Schneider. Solid particle erosion behavior of nanolaminated Cr_2AlC films // *Wear*. 2018, v. 402-403, p. 187-195.

42. A. Anders. A structure zone diagram including plasma-based deposition and ion etching // *Thin Solid Films*. 2010, v. 518, p. 4087-4090.

43. N. Laska, P. Bauer, O. Helle, F. Kreps. Sputtering and Characterization of MAX-Phase Forming Cr–Al–C and Ti–Al–C Coatings and Their Application on γ-Based Titanium Aluminides // *Adv. Eng. Mater*. 2022, v. 24, p. 2100722.

44. J. Liu, X. Zuo, Z. Wang, L. Wang, X. Wu, P. Ke, A. Wang. Fabrication and mechanical properties of high purity of Cr_2AlC coatings by adjustable Al contents // *J. Alloys and Compounds*. 2018, v. 753, p. 11-17.

45. S. Heinze, A. Stark, J. Hendl, C. Leyens. Influence of the deposition process on the Cr_2AlC phase formation during heat treatment of Cr-Al-C thin films // *Materials and Design*. 2023, v. 225, p. 111462.

46. Z. Wang, G. Ma, L. Liu, L. Wang, P. Ke, Q. Xue, A. Wang. High-performance Cr_2AlC MAX phase coatings: Oxidation mechanisms in the 900…1100 °C temperature range // *Corrosion Science*. 2020, v. 167, p. 108492.

47. M.W. Barsoum. The $M_{n+1}AXn$: a new class of solids; thermodynamically stable nanolaminates // *Prog. Solid St. Chem.* 2000, v. 28, p. 201-281.

48. C. Walter, D.P. Sigumonrong, T. El-Raghy, J.M. Schneider. Towards large area deposition of

Cr_2AlC on steel // *Thin Solid Films*. 2006, v. 515, N 2, p. 389-393.

49. J.M. Schneider, Z.M. Sun, R. Mertens, F. Uestel, R. Ahuja. Ab initio calculations and experimental determination of the structure of Cr_2AlC // *Solid State Commun.* 2004, v. 130, N 7, p. 445-449.

50. J. Emmerlich, H. Högberg, S. Sasvári, P.O.Å. Persson, L. Hultman, J.P. Palmquist, U. Jansson, J.M. Molina-Aldareguia, Z. Czigány. Growth of Ti_3SiC_2 thin films by elemental target magnetron sputtering // *J. Appl. Phys.* 2004, v. 96, N 9, p. 4817-4826.

51. J.P. Palmquist, U. Jansson, T. Seppänen, P.O.Å. Persson, J. Birch, L. Hultman, P. Isberg. Magnetron sputtered epitaxial single-phase Ti_3SiC_2 thin films // *Appl. Phys. Lett.* 2002, v. 81, N 5, p. 835-837.

52. J.P. Palmquist, S. Li, P.O.Å. Persson, J. Emmerlich, O. Wilhelmsson, H. Högberg, M.I. Katsnelson, B. Johansson, R. Ahuja, O. Eriksson, L. Hultman, U. Jansson. $M_{n+1}AX_n$ phases in the Ti-Si-C system studied by thin-film synthesis and ab initio calculations // *Phys. Rev. B*. 2004, v. 70, N 6, p. 165401.

53. H. Högberg, P. Eklund, J. Emmerlich, J. Birch, L. Hultman. Epitaxial Ti_2GeC, Ti_3GeC2, and Ti_4GeC_3 MAX-phase thin films grown by magnetron sputtering // *J. Mater. Res.* 2005, v. 20, p. 779.

54. A.S. Ingason, A. Petruhins, J. Rosen. Toward Structural Optimization of MAX Phases as Epitaxial Thin Films // *Mater. Res. Lett.* 2016, v. 4, p. 152-160.

55. M. Beckers, N. Schell, R.M.S. Martins, A. Mücklich, W. Möller. Phase stability of epitaxially grown Ti_2AlN thin films // *Appl. Phys. Lett.* 2006, v. 89, p. 074101.

56. J. Yuan, Z. Wang, G. Ma, X. Bai, Y. Li, X. Cheng, P. Ke, A. Wang. MAX phase forming mechanism of M–Al–C (M = Ti, V, Cr) coatings: In-situ X-ray diffraction and first-principle calculations // *J. Mater. Sci. Technol*. 2023, v. 143, p. 140-152.

57. T.F. Zhang, Q.M. Wang, J. Lee, P. Ke, R. Nowak, K.H. Kim. Nanocrystalline thin films synthesized from a Ti_2AlN compound target by high power impulse magnetron sputtering technique // *Surf. Coatings Technol.* 2012, v. 212, p. 199-206.

58. O. Berger, C. Leyens, S. Heinze, R. Boucher, M. Ruhnow. Characterization of Cr–Al–C and Cr–Al–C–Y films synthesized by High Power Impulse Magnetron Sputtering at a low deposition temperature // *Thin Solid Films*. 2015, v. 580, p. 6-11.

59. A.I. Kalinichenko, E. Reshetnyak, V. Strel'nitskij, G. Abadias. Role of nonlocal thermoelastic peaks in the stress and texture evolution of TiN coatings formed by plasma based ion implantation and deposition // *Surface and Coatings Technology*. 2020, v. 391, p. 125695.

60. G. Abadias. Stress and preferred orientation in nitride-based PVD coatings // *Surf. Coat. Technol.* 2008, v. 202, N 11, p. 2223-2235.

61. J. Wang, J. Wang, Y. Zhou. Stable M_2AlC (0001) surfaces (M = Ti, V and Cr) by first-principles investigation // *J. Physics: Condens. Matter.* 2008, v. 20, N 22, p. 225006.

62. G. Ma, D. Zhang, P. Guo, H. Li, Y. Xin, Z. Wang, A. Wang. Phase orientation improved the corrosion resistance and conductivity of Cr_2AlC coatings for metal bipolar plates // *J. Mater. Sci. Technol.* 2022, v. 105, p. 36-44.

63. M.A. Bortnitskaya, E.N. Reshetnyak, A.S. Kuprin, T.A. Prikhna, V.B. Sverdun, I.V. Kolodiy, V.A. Belous, V.G. Marinin, T.B. Serbenyuk. Structure and Mechanical Characteristics of Ti_2AlC MAX phase cathodes and deposited ion-plasma coatings // *J. Nano- and Electronic Physics*. 2021, v. 13, N 5, p. 05031 (7).

64. Z. Wang, X. Li, J. Zhou, P. Liu, Q. Huang, P. Ke, A. Wang. Microstructure evolution of V-Al-C coatings synthesized from a V_2AlC compound target after vacuum annealing treatment // *J. Alloys and Compounds.* v. 661, p. 476-482.

65. A. Cavaleiro. *Nanostructured Coatings* / J.T.De Hosson (Eds.). New York: Springer, 2006, 648 p.

66. S.B. Li, W.B. Yu, H.X. Zhai, G.M. Song, W.G. Sloof, S. van der Zwaag. Mechanical properties of low temperature synthesized dense and finegrained Cr_2AlC ceramics // *J. Eur. Ceram. Soc*. 2011, v. 31, p. 217-224.

67. Q. Yang, R. McKellar. Nanolayered CrAlTiN and multilayered CrAlTiN–AlTiN coatings for solid particle erosion protection // *Tribol. Int.* 2015, v. 83, p. 12-20.

68. B. Borawski, J. Singh, J.A. Todd, D.E. Wolfe, Multi-layer coating design architecture for optimum particulateerosion resistance // *Wear.* 2011, v. 271, p. 2782-2792.

69. J. Emmerlich, G. Gassner, P. Eklund, et al. Micro and macroscale tribological behavior of epitaxial Ti_3SiC_2 thin films // *Wear*. 2008, v. 264, p. 914-919.

70. O. Wilhelmsson, M. Råsander, M. Carlsson, et al. Design of nanocomposite low-friction coatings // *Adv. Funct. Mater*. 2007, v. 17, p. 1611-1616.

71. S. Gupta, D. Filimonov, V. Zaitsev, T. Palanisamy, M.W. Barsoum, Ambient and 550 °C tribological behavior of select MAX phases against Ni-based superalloys // *Wear*. 2008, v. 264, p. 270-278.

72. S. Gupta, D. Filimonov, T. Palanisamy, T. El-Raghy, M.W. Barsoum. Ta_2AlC and Cr_2AlC Ag-based composites-New solid lubricant materials for use over a wide temperature range against Ni-based superalloys and alumina // *Wear.* 2007, v. 262 (11-12), p. 1479-1489.

73. S. Gupta, D. Filimonov, T. Palanisamy, M.W. Barsoum. Tribological behavior of select MAX phases against Al_2O_3 at elevated temperatures // *Wear.* 2008, v. 265 (3-4), p. 560-565.

74. J.H. Ouyang, S. Sasaki. Effects of different additives on microstructure and high-temperature tribological properties of plasma-sprayed Cr_2O_3 ceramic coatings // *Wear*. 2001, v. 249 (1-2), p. 56-66.

75. J. Gonzalez-Julian, J. Llorente, M. Bram, M. Belmonte, O. Guillon. Novel Cr_2AlC MAX-phase/SiC fiber composites: Synthesis, processing and tribological response // *J. Eur. Ceram. Soc*. 2017, v. 37(2), p.467-475.

76. R. Pei, S.A. McDonald, L. Shen, S. van der Zwaag, W.G. Sloof, P.J. Withers, P.M. Mummery. Crack healing behaviour of Cr_2AlC MAX phase studied by X-ray tomography // *J. Eur. Ceram. Soc.* 2017, v. 37, p. 441-450.

77. S.B. Li, L.O. Xiao, G.M. Song, X.M. Wu, W.G. Sloof, S. van der Zwaag. Oxidation and crack healing behavior of a fine-grained Cr_2AlC ceramic // *J. Am. Ceram. Soc.* 2013, v. 96, p. 892-899.

78. H.J. Yang, Y.T. Pei, J.Th.M. De Hosson. Oxide-scale growth on Cr_2AlC ceramic and its consequence for self-healing // *Scr. Mater.* 2013, v. 69, p. 203-206.

79. H.J. Yang, Y.T. Pei, J.C. Rao, J.Th.M. De Hosson. Self-healing performance of Ti_2AlC ceramic // *J. Mater. Chem*. 2012, v. 22, p. 8304.

80. G.P. Bei, B.-J. Pedimonte, T. Fey, P. Greil. Oxidation behavior of MAX phase $Ti_2Al_{(1-x)}Sn_xC$ solid solution // *J. Am. Ceram. Soc.* 2013, v. 96, p. 1359-1362.

81. Z. Wang, J. Sun, B. Xu, Y. Liu, P. Ke, A. Wang. Reducing the self-healing temperature of Ti_2AlC MAX phase coating by substituting Al with Sn // *J. Eur. Ceram. Soc.* 2020, v. 40, p. 197-201.

82. B. Liu, J.Y. Wang, J. Zhang, J.M. Wang, F.Z. Li, Y.C. Zhou. Theoretical investigation of A-element atom diffusion in Ti_2AlC (A=Ga, Cd, In, and Pb) // *Appl. Phys. Lett.* 2009, v. 94, p. 181906.

83. T. Zhanga, H. Myounga, D. Shinc, K. H. Kima. Syntheses and properties of Ti_2AlN MAX-phase films // *J. Ceram. Process. Res.* 2012, v. 13, N S1, p. 149-153.

84. S. Mraz, M. Tyra, M. to Baben, M. Hans, X. Chen, F. Herrig, K. Lambrinou, J.M. Schneider. Thermal stability enhancement of Cr_2AlC coatings on Zr by utilizing a double layer diffusion barrier // *J. Eur. Ceram. Soc.* 2020, v. 40, N 4, p. 1119-1124.

85. Q.M. Wang, A. Flores Renteria, O. Schroeter, R. Mykhaylonka, C. Leyens, W. Garkas, M. to Baben. Fabrication and oxidation behavior of Cr_2AlC coating on Ti6242 alloy // *Surf. Coat. Technol*. 2010, v. 204, N 15, p. 2343-2352.

86. J.J. Li, M.S. Li, H.M. Xiang, X.P. Lu, Y.C. Zhou. Short-term oxidation resistance and degradation of Cr_2AlC coating on M38G superalloy at 900-1000°C // *Corrosion Sci.* 2011, v. 53, p. 3813-3820.

87. T.A. Prikhna, O.P. Ostash, A.S. Kuprin, V.Ya. Podhurska, T.B. Serbenyuk, E.S. Gevorkyan, M. Rucki, W. Zurowski, W. Kucharczyk, V.B. Sverdun, M.V. Karpets, S.S. Ponomaryov, B.D. Vasyliv, V.E. Moshchil, M.A. Bortnitskaya. A new MAX phases-based electroconductive coating for high-temperature oxidizing environment // *Composite Structures*. 2021, v. 277, p. 114649.

88. V. Podhurska, O. Kuprin, T. Prikhna, O. Ostash, D. Pohl, M. Karpets, V. Sverdun, T. Serbeniuk, R. Chepil, P. Potapov, S. Ponomarov. Development of oxidation-resistant and electrically conductive coating of Ti–Al–C system for the lightweight interconnects of solid oxide fuel cells // *Heliyon*. 2024, v. 10, N 1, e23275.

89. X. Chen, B. Stelzer, M. Hans, R. Iskandar, J. Mayer, J.M. Schneidera. Enhancing the high temperature oxidation behavior of Cr_2AlC coatings by reducing grain boundary nanoporosity // *Mater. Res. Lett.* 2020, v. 9, N 3, p. 127-133.

90. J. Fu, T.F. Zhang, Q. Xia, S-H. Lim, Z. Wan, T.W. Lee, K.H. Kim. Oxidation and Corrosion Behavior of Nanolaminated MAX-Phase Ti_2AlC Film Synthesized by High-Power Impulse Magnetron Sputtering and Annealing // *Journal of Nanomaterials*. 2015, v. 2015, Article ID 213128, 12 p.

91. W. Li, Z. Wang, J. Shuai, B. Xu, A. Wang, P. Ke. A high oxidation resistance Ti_2AlC coating on Zirlo substrates for loss-ofcoolant accident conditions // *Ceram. Int.* 2019, v. 45, p. 13912-13922.

92. C. Tang, M. Steinbrueck, M. Stueber, M. Grosse, X. Yu, S. Ulrich, H.J. Seifert. Deposition, characterization and high-temperature steam oxidation behavior of single-phase Ti_2AlC-coated Zircaloy-4 // *Corrosion Science.* 2018, v. 135, p. 87-98.

93. L. Gröner, L. Mengis, M. Galetz, L. Kirste, P. Daum, M. Wirth, F. Meyer, A. Fromm, B. Blug, F. Burmeister. Investigations of the Deuterium Permeability of As-Deposited and Oxidized Ti_2AlN Coatings // *Materials*. 2020, v. 13, p. 2085.

94. D.E. Hajas, M. Scholz, S. Ershov, B. Hallstedt, J.-P. Palmquist, J.M. Schneider. Thermal and chemical stability of Cr_2AlC in contact with α-Al_2O_3 and NiAl // *Int. J. Mater. Res.* 2010, v. 101, p. 1519-1523.

95. M. Sokol, J. Yang, H. Keshavan, M.W. Barsoum, Bonding and oxidation protection of Ti_2AlC and Cr_2AlC for a Ni-based superalloy // *J. Eur. Ceram. Soc*. 2019, v. 39, p. 878-882.

96. J. Zhang, Z. Tian, H. Zhang, L. Zhang, J. Wang. On the chemical compatibility between Zr-4 substrate and well-bonded Cr_2AlC coating // *J. Mater. Sci. Technol*. 2019, v. 35, p. 1-5.

97. M. Haftani, M.S. Heydari, H.R. Baharvandi, N. Ehsani. Studying the oxidation of Ti_2AlC MAX phase in atmosphere: a review // *Int. J. Refract. Metals Hard Mater.* 2016, v. 61, p. 51-60.

98. X.K. Qian, X.D. He, Y.B. Li, Y. Sun, H. Li, D.L. Xu, Cyclic oxidation of Ti_3AlC_2 at 1000–1300 °C in air // *Corros. Sci.* 2011, v. 53, p. 290-295.

99. D.J. Tallman, B. Anasori, M.W. Barsoum. A critical review of the oxidation of Ti_2AlC, Ti_3AlC_2 and Cr_2AlC in Air // *Mater. Res. Lett*. 2013, v.1, N 3, p. 115-125.

100. C. Tang, M. Steinbrück, M. Grosse, S. Ulrich, M. Stüber. The Effect of Annealing Temperature on the Microstructure and Properties of Cr–C–Al Coatings on Zircaloy-4 for Accident-Tolerant Fuel (ATF) Applications // *Coatings.* 2022, v. 12, p. 167.

101. C. Tang, M. Große, S. Ulrich, M. Klimenkov, U. Jäntsch, H.J. Seifert, M. Stüber, M. Steinbrück. High-temperature oxidation and hydrothermal corrosion of textured Cr_2AlC-based coatings on zirconium alloy fuel cladding // *Surface and Coatings Technology*. 2021, v. 419, p. 127263.

102. J.L. Lu, N. Abbas, J.N. Tang, J. Tang, G.M. Zhu. Synthesis and characterization of conductive ceramic MAX-phase coatings for metal bipolar plates in simulated PEMFC environments // *Corrosion Science*. 2019, v. 158, p. 108106.

103. J.L. Lu, N. Abbas, J. Tang, R. Hu, G.M. Zhu. Characterization of Ti_3SiC_2-coating on stainless steel bipolar plates in simulated proton exchange membrane fuel cell environments // *Electrochemistry Communications*. 2019, v. 105, p. 106490.

104. J.G. Gigax, M. Kennas, H. Kim, T. Wang, B.R. Maier, H. Yeom, G.O. Johnson, K. Sridharan,

L. Shao. Radiation response of Ti_2AlC MAX phase coated Zircaloy-4 for accident tolerant fuel cladding // *Journal of Nuclear Materials*. 2019, v. 523, p. 26-32.

105. V.N. Voyevodin, G.D. Tolstolutskaya, M.A. Tikhonovsky, A.S. Kuprin, A.S. Kalchenko. Mechanisms of radiation damage and development of structural materials for operating and advanced nuclear reactors // *Problems of Atomic Science and Technology*. 2021, N 5(135), p. 3-20.

106. M. Bugnet, V. Mauchamp, E. Oliviero, M. Jaouen, T. Cabioc'h. Chemically sensitive amorphization process in the nanolaminated Cr_2AC (A = Al or Ge) system from TEM in situ irradiation // *Journal of Nuclear Materials*. 2013, v. 441, N 1–3, p. 133-137.

107. M. Imtyazuddin, A.H. Mir, M.A. Tunes, V.M. Vishnyakov. Radiation resistance and mechanical properties of magnetron-sputtered Cr_2AlC thin films // *Journal of Nuclear Materials*. 2019, v. 526, p.151742.

108. M. Imtyazuddin, A.H. Mir, E. Aradi, V. Vishnyakov. Effect of aluminium concentration on phase formation and radiation stability of Cr_2Al_xC thin film // *Nanotechnology*. 2020, v. 31, N 38, p. 385602.

109. M.A. Tunes, M. Imtyazuddin, C. Kainz, S. Pogatscher, V.M. Vishnyakov. Deviating from the pure MAX phase concept: Radiation-tolerant nanostructured dual-phase Cr_2AlC // *Science Advances*. 2021, v. 7, N 13, eabf6771 (1-12 p.).

110. C. Wang, Z. Han, R. Su, J. Gao, L. Shi. Effects of irradiation damage on the structure in Cr_2AlC thin film // *Nucl. Instrum. Meth. in Phys. Res. Section B: Beam Interactions with Materials and Atoms*. 2019, v. 450, p. 286-290.

111. C. Wang, H. Tu, R. Su, J. Gao, B.V. King, D.J. O'Connor, L. Shi. Annealing effects on the structure and hardness of helium-irradiated Cr_2AlC thin films // *Journal of the American Ceramic Society*. 2021, v. 104, N 1, p. 593-603.

112. R. Su, H. Zhang, L. Liu, L. Shi, H. Wen. Reversible phase transformation in Ti_2AlC films during He radiation and subsequent annealing // *Journal of the European Ceramic Society*. 2021, v. 41, N 13, p. 6309-6318.

113. W. Ling, K. Lai, J. Chen, F. Guo, D. Kang, Z. Zhao, J. Dai. Point defects and hydrogen-permeation behavior of MAX phase Cr_2AlC coating by first-principles studies // *Nuclear Materials and Energy*. 2023, v. 36, p. 101486.

114. C. Tang, M. Grosse, P. Trtik, M. Steinbrueck, M. Stueber, H.J. Seifert. H_2 permeation behavior of Cr_2AlC and Ti_2AlC max phase coated Zircaloy-4 by neutron radiography // *Acta Polytechnica*. 2018, v. 58, N 1, p. 69-76.

Article received 20.03.2024

СИНТЕЗ, СТРУКТУРА ТА ЗАХИСНІ ВЛАСТИВОСТІ PVD-ПОКРИТТІВ МАХ-ФАЗ. ОГЛЯД. ЧАСТИНА II. СТРУКТУРА, ВЛАСТИВОСТІ, ПЕРСПЕКТИВИ ЗАСТОСУВАННЯ

О.М. Решетняк, О.С. Купрін, Т.О. Пріхна, М.О. Бортницька, В.А. Білоус

Унікальні гібридні властивості кераміки та металів, що обумовлені особливою наношаруватою структурою, роблять МАХ-фази привабливим матеріалом для роботи у жорстких умовах. Успіхи у розробці PVD-процесів синтезу нанокристалічних покриттів МАХ-фаз при знижених температурах на технологічно значущих підкладках відкривають значні перспективи їх застосування. Дана частина огляду присвячена розгляду властивостей МАХ-фаз, які роблять їх корисними для створення мультифункціональних покриттів і захисту поверхні матеріалів, що працюють у складних умовах дії високої температури, корозії та радіації. Проаналізовано вплив параметрів PVD-осадження на структуру покриттів МАХ-фаз. Обговорюються особливості механічних і трибологічних властивостей покриттів, їх стійкість до ерозії, корозії та радіаційного опромінення, здатність до самовідновлення пошкоджень при високих температурах. Розглянуто перспективи застосування PVD-покриттів на основі МАХ-фаз у різних галузях та способи покращення їх захисних властивостей.